

4. SITE 220

The Shipboard Scientific Party¹
 With Additional Reports From
 Robert Coleman, U. S. Geological Survey, Menlo Park, California
 and
 Norman Hamilton, University of Southampton, United Kingdom

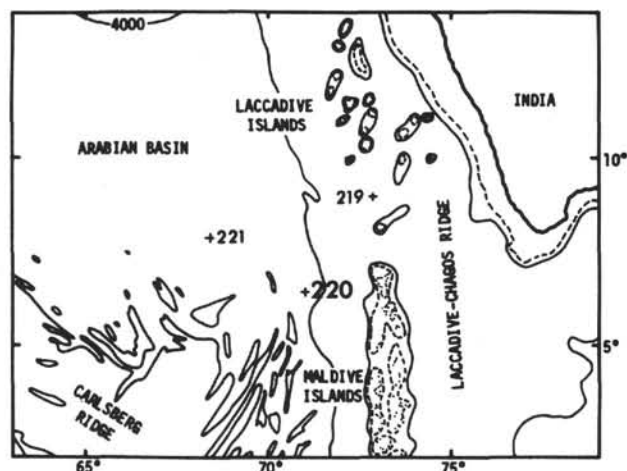


Figure 1. Position of Site 220 and adjacent Leg 23 sites (shown by +). Contours at 200, 1000, and 4000 meters from Laughton et al. (1971).

SITE DATA

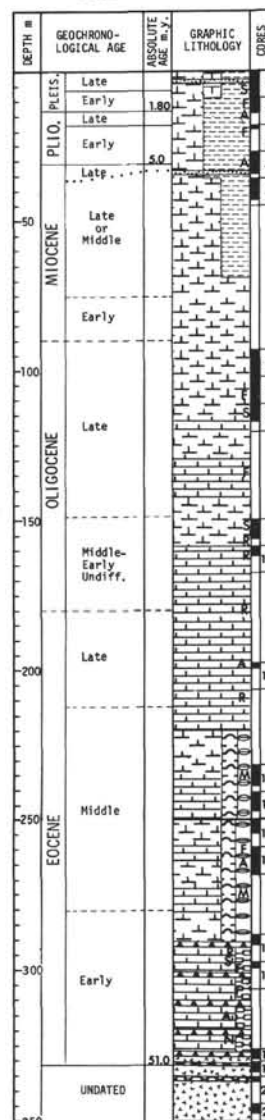
Dates: 1950 14 Mar–0550 17 Mar 72
 Time: 58 hours
 Position (Figure 1): 6°30.97'N, 70°59.02'E
 Holes Drilled: 1
 Water Depth by Echo-Sounder: 4036 corr. meters
 Total Penetration: 350 meters
 Total Core Recovered: 100.9 meters from 21 cores
 Age of Oldest Sediment: Early Eocene
 Basement: Basalt

ABSTRACT

A complete penetration of Pleistocene through Lower Eocene strata plus underlying oceanic basalt was recorded at this site. Nannofossil oozes and chinks dominate almost the entire 51 m.y. period of deep-water sediment accumulation. The Eocene sediments record the deposition of large amounts of radiolarians and sponge spicules which through diagenetic change developed into a deep-lying chert reflector. Neogene strata contain foraminiferal sands which helped construct local abyssal plain topography in this region.

¹Robert B. Whitmarsh, National Institute of Oceanography, Wormley, Godalming, Surrey, United Kingdom; Oscar E. Weser, Scripps Institution of Oceanography, La Jolla, California; Syed Ali, State University of New York, Stony Brook, New York; Joseph E.

SITE SUMMARY



Boudreaux, Texaco Inc., New Orleans, Louisiana; Robert L. Fleisher, University of Southern California, Los Angeles, California; Dan Jipa, M.I.M.G. Institutul Geologic, Bucharest, Romania; Robert B. Kidd, Southampton University, Southampton, United Kingdom (Present address: National Institute of Oceanography, Wormley, Godalming, Surrey, United Kingdom); Tapas K. Malik, Geological Survey of India, Calcutta, India; Albert Matter, Geologisches Institut, Universität Bern, Bern, Switzerland; Catherine Nigrini, Lexington, Massachusetts; Hassan N. Siddiquie, Geological Survey of India, Calcutta India (Present address: National Institute of Oceanography, Goa, India); Peter Stoffers, Laboratorium für Sedimentforschung, Universität Heidelberg, Heidelberg, Germany.

BACKGROUND AND OBJECTIVES

The sea floor spreading history of the Indian Ocean since the Late Cretaceous has recently been described by McKenzie and Sclater (1971). Their study was based on shipborne and airborne magnetic anomaly profiles which they analyzed and correlated in order to determine rates of past sea floor spreading and the former trends of the sea floor spreading ridges. The work of McKenzie and Sclater included the northwest Indian Ocean. In this region, it was usually possible to identify anomalies 3 and 5 on either side of the Carlsberg Ridge, although immediately east of the Owen Fracture Zone, these anomalies could not be distinguished, probably because of the proximity of the geomagnetic equator at this latitude. As a result of these anomaly identifications, a mean spreading rate of 1.2 to 1.3 cm/yr was determined for the last 10 m.y. Beyond anomaly 5, McKenzie and Sclater recognized a "quiet magnetic zone" with few anomalies extending to a region of large distinctive magnetic anomalies, the youngest of which is anomaly 23 (58 m.y. old). North of the Carlsberg Ridge, these older anomalies trend east-west and were formed at a spreading rate of 6.5 cm/yr. From the magnetic data, therefore, it is not possible at present to determine the spreading history of the Arabian Sea for the interval 10 to 58 m.y., which represents a large part of Tertiary time. However, McKenzie and Sclater invoked theoretical calculations which explain the increasing depth of the basaltic basement away from spreading ridges in terms of cooling of the lithospheric plate. The agreement between the observed bathymetry and that arrived at from such calculations suggests that the most recent spreading episode began as early as 35 m.y. ago. Before that time, these authors postulate that there was an interval of very slow or no spreading for 20 m.y. Clearly this hypothesis, based on broad average features of the bathymetry and on calculations insensitive to small changes in spreading rate, is ideally suited to the test of the drill and for this reason a prospective Site 220 was sought for in the area of unidentified magnetic anomalies between anomalies 5 and 23.

The choice of position for Site 220 was severely limited by the availability of seismic reflection profiles, only two of which were known to fit the above constraint north of the Carlsberg Ridge (Ewing et al., 1969). A suitable site was found on the *Conrad-9* profile (Figure 2) where it crossed a broad platform at about 4000 meters on the west flank of the Maldivian mass. Although anomaly 23 had not been identified north of this site, the interpretation of McKenzie and Sclater (loc. cit. fig. 50a) put the site well within the interval 10-38 m.y. On this part of the seismic profile, the acoustic basement is irregular but without the jagged character of the present-day Carlsberg Ridge. The saw-tooth basement profile, with eastward facing scarps, suggests normal faulting and is similar to the disposition of the Eocene cherts near Site 219. Overlying the basement unconformably, there is a transparent layer between 0.2 to 0.6 sec thick with a westward component of dip. The layer contains two weak reflectors. This transparent layer outcrops to the east and west of the site, forming rather flat-topped hills. A horizontally stratified layer (turbidites?), 0.15 to 0.2 sec thick, unconformably overlies the transparent layer, and its top forms an almost flat sea bed.

To the south and west of Site 220, north-northeast to northeast trending ridges traverse the sea floor from the crest of the Carlsberg Ridge. East of the longitude of the site, however, they merge into the uniform west slope of the Maldives. Slightly northwest of the site these ridges disappear from the sea floor, probably as a result of blanketing by the turbidites of the Arabian Abyssal Plain, in which case, the northward subbottom extension of the ridges cannot be ruled out. It seems that these ridges are continuations of the northeast striking fracture zones which offset the axis of the Carlsberg Ridge south of 3°N (Fisher et al., 1971).

A reversed seismic refraction line, shot in depths around 3900 meters, 140 km to the north of Site 220, yielded a normal oceanic crustal structure with a total thickness of 9 to 10 kms (Francis and Shor, 1966). Thus, it is highly likely that Site 220, in a similar depth of water, has a similar normal crustal structure and thickness.

Thus, the objectives of drilling this site were to:

- 1) Sample and date the igneous basement in order to put a constraint on the spreading history of the Arabian Sea in the period 10 to 58 m.y. ago.
- 2) Determine the history of the site from the sediments, especially the age of the uppermost unconformity.
- 3) Obtain paleomagnetic samples for paleolatitude determinations ashore.

The JOIDES Advisory Panel on Pollution Prevention and Safety imposed an operational constraint on drilling at this site that all reflectors should be cored.

OPERATIONS

Site 220 was approached from the northeast along a track slowly converging with the *Conrad-9* track, from which the proposed site had been chosen. In view of the cherty nature of the main reflector at Site 219, and the similar character of the *Conrad-9* profile over the proposed position of Site 220, it was decided to choose a site where the main reflector was as close as possible to the sea bed. This was done to save drilling time in case a thick sedimentary sequence lay below the chert and above igneous basement. Such a sequence, and indeed the basement itself, could probably remain undetected due to the masking effect of the strong chert reflector. Consequently, the aim of the presite survey was to locate a place where the uppermost stratified layer (turbidites?) was at its thinnest but to avoid hilly areas which might not provide sufficient soft sediment to bury the bottom hole assembly.

Another objective of the survey was to discover the trend, if any, of the low hills and associated irregularities of the basement surface. Since this trend was expected to be NNE, parallel to the ridges and troughs mapped to the southwest on bathymetric charts, a Z-shaped presite survey was carried out to pick up trends in this direction. In fact, two additional tracks, plus data obtained on leaving the site, showed that the trend of the hill close to the site was northwest.

Site 220 was chosen on the southwest flank of a 100-meter-high hill after a site survey, which had taken 4½ hours at a speed of 8 knots. The 16 kHz beacon was dropped at 0052 hours 15 March while *Glomar Challenger* was underway at 5 knots. Navigation during the survey had

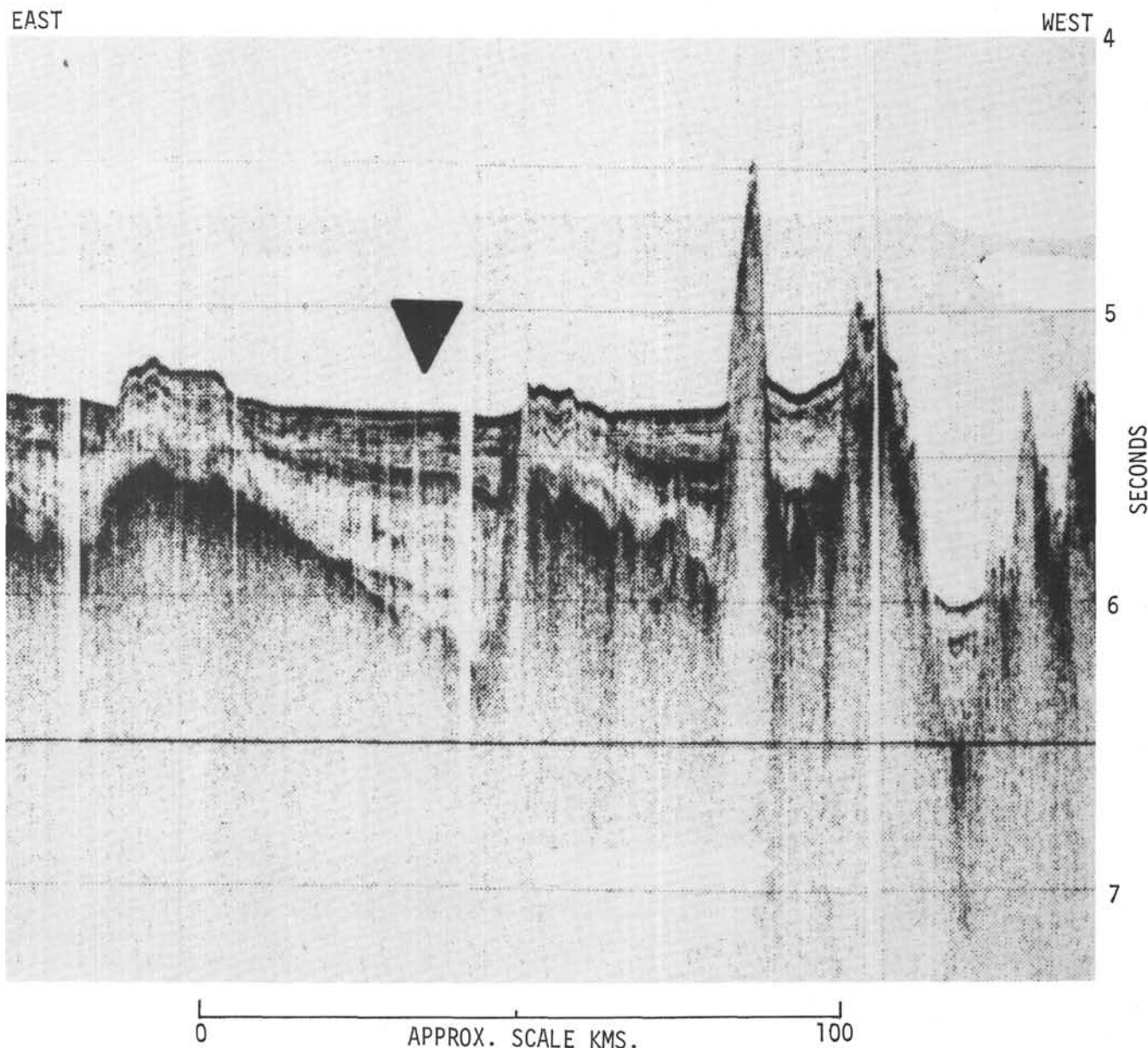


Figure 2. Seismic reflection profile across the proposed position of Site 220 (arrowed). The eventual site position was just west of the seamount in the center of the figure. Profile from cruise Conrad-9 courtesy of the Lamont-Doherty Geological Observatory.

been hampered by a lack of satellite fixes, and the dead reckoned course was subject to a surface current with an easterly component of about 0.7 knots. After all gear had been brought onboard, the ship returned to the beacon and took up station. An offset of 500 meters in the direction 115° was effected almost immediately since the depth under the ship was less than that during the first passover the site, but, in fact, the depth shoaled even further. Consequently, the ship returned to a position directly over the beacon and drilling operations began.

Keeping in mind the main objective of sampling basement, a drilling program of mostly intermittent coring was followed (Table 1). Because of an interest in the shallowest sediments, Cores 1 to 5 (0 to 45 m) were taken continuously. The first core at the surface was a punch core. For the second core it was decided to replace

the plastic liner with the split metal liner designed for use in the Red Sea hot brine area. When brought upon deck and opened, this liner was half full, and the only problem in removing the sediments was their adhesion to the metal. The test of the metal liner was considered successful. Below Core 5, the sediments were alternately cored and drilled, with 20- to 48-meter drilled intervals separating the cores, to a depth of 306 meters. Circulation was first broken in nanno oozes at Core 7 and intermittently thereafter; it was particularly necessary with the advent of chalk, which was first encountered in Core 8. With the beginning of occasional chert stringers in Core 12, the bit weight had to be increased in steps from 10,000 to 20,000 lb. Near Core 14 dips of up to 45° appeared in the split cores. The drillers considered it most unlikely that this phenomenon could be due to a nonvertical hole.

TABLE 1
Coring Summary, Site 220

Core	Date/Time Core on Deck (Time Zone-5)	Depth Below Sea Floor (m)	Cored (m)	Recovered (m)
15 Mar:				
1 ^a	1020	0-9	9.0	8.5
2 ^b	1125	9-18	9.0	4.5
3 ^c	1237	18-27	9.0	CC
4	1350	27-36	9.0	7.0
5	1500	36-45	9.0	6.4
6	1705	93-102	9.0	9.4
7 ^d	1815	102-111	9.0	9.3
8	1930	111-120	9.0	6.2
9	2115	150-159	9.0	5.6
10	2225	159-168	9.0	2.8
16 Mar:				
11	0005	198-207	9.0	1.5
12	0200	232-241	9.0	7.3
13	0315	241-250	9.0	5.6
14	0435	250-259	9.0	4.5
15	0555	259-268	9.0	8.0
16 ^e	0745	288-297	9.0	2.0
17	0915	297-306	9.0	1.5
18	1300	326-300	4.0	4.9
19	1550	330-335	5.0	2.5
20	2020	335-344	9.0	0.5
17 Mar:				
21	0045	344-350	6.0	2.9
Totals			177.0	100.9

^aObtained with extended core barrel.

^bMetal liner used inside core barrel.

^cExtended core barrel.

^dPumps on, mostly intermittently from here.

^eCoring time over 20 min from here, pumps on continually.

The drilling rate decreased rapidly when basalt was encountered in Core 18. Approximately 7 meters of basalt were recovered from a 20-meter interval of basalt penetration. Mud was spotted in the hole to remove any cuttings when the bit began to torque up. Also, there was a suggestion of damage to the roller cones on the bit because of the extremely slow coring rate (as little as 2.4 m/hr) and the undergauge core material. Although slight further penetration could have been possible, all geological objectives had been reached, and it was decided to abandon the hole after Core 21 had been recovered from a terminal depth of 350 meters.

Upon examining the drill bit on the drill floor, several teeth of the roller cones were seen to be broken, apparently by the chert stringers. Additionally, the sealed bearings were badly worn and the cones were slightly askew, restricting the flow of fluid through the jets.

An airgun profile passing directly over the beacon was obtained at 8 knots on leaving the site. This profile, and a further profile at full speed, supplemented the presite survey and enabled a contoured bathymetric chart to be constructed of the area around the site (Figure 3).

LITHOLOGY

Hole 220 penetrated 350 meters below the sea bed. Some of the intervals were drilled without coring and the longest uncored gap was 48 meters. Strata encountered at

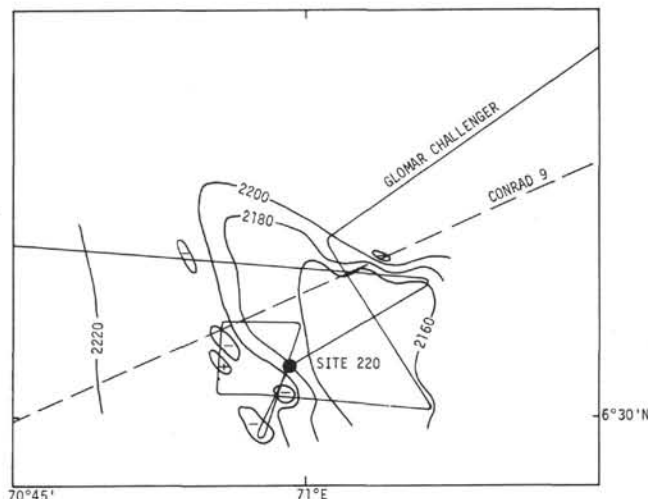


Figure 3. Bathymetric chart of the area around Site 220 based on the tracks of Glomar Challenger and Conrad. Contour interval is 20 fms, depths in corrected fathoms. Conrad data kindly provided by D. E. Hayes, Submarine Topography Department, Lamont-Doherty Geological Observatory.

the site can be divided into 5 major units on the bases of visual examination, compositional variations noted on smear slides, and the results of carbonate analyses. The lithologic units are summarized in Table 2.

Unit I

The sediments are soft and massive and consist of orange to brown nanno detrital clay with intervals of detrital clay nanno ooze. Clay amounts to nearly 45 percent of the sediment constituents. The sediments are occasionally glass, foram, or spicule bearing and in Core 1 they are foram rich. The carbonate percentage varies between 11 and 67 percent and averages 50 percent (see Figure 4). There seems to be a decrease in the carbonate percentage in the basal part of the unit. The bulk X-ray sample from Core 4, a typical unit I lithology, shows high amounts of calcite (47%), quartz (17%), and mica (16%). Thin foram sand layers with sharp upper and lower bedding contacts can be distinguished at intervals in Cores 1 and 4. Additional unsampled intervals in unit I are probably foram sands also.

Unit II

Unit II sediments differ from those of unit I by their almost complete absence of clay particles, a white color, and the gradual appearance of well-bedded chalk intervals alternating with the ooze. This unit accounts for almost one-half of the sedimentary column at this site. Nanno chalk bands are of varying thickness (1 to 12 cm) and they and the nanno ooze contain about 95 percent nannofossils. The unit is locally sponge spicule, foram- or rad-bearing and sometimes volcanic glass rich. Minor amounts of needle-like carbonate particles are present, which, by analogy with those reported by von Stackelberg (1972) in this area, are probably aragonitic. The unit contains a high percentage of carbonates, 89 percent on the average (see Figure 4).

TABLE 2
Lithologic Summary, Site 220

Lithologic Units		Thickness (m)	Subbottom Depth (m)	Cores
I	Orange to brown NANNO DETRITAL CLAY and DETRITAL CLAY NANNO OOZE. Few FORAM SAND beds	ca. 69	0-69	1-5
II	White NANNO OOZE and CHALK	ca. 151	69-220	6-11
III	Light orange RAD SPICULE RICH NANNO OOZE/CHALK with thin ASH beds	ca. 70	220-290	12-16
IV	Light orange MICARB-RICH NANNO CHALK with thin CHERT beds	39	290-329	16-18
V	BASALT flows with thin interbedded sediment layers	21	329-350	18-21

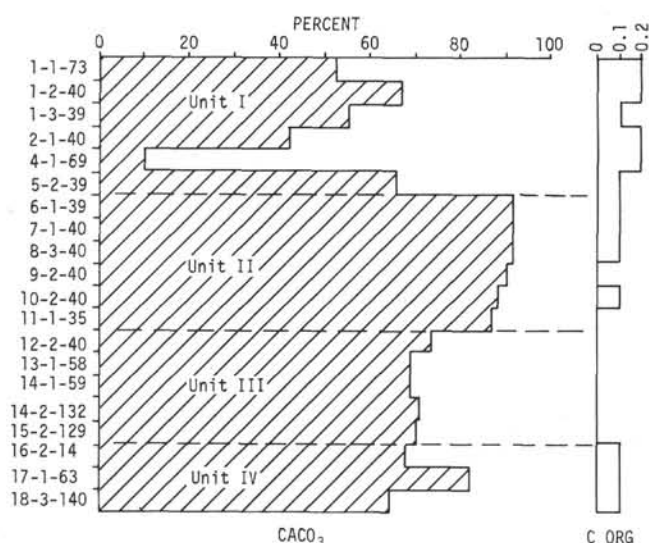


Figure 4. Distribution of calcium carbonate and organic carbon in lithological units I through IV.

Unit III

The change from unit II lithology into the pale orange rad spicule-rich micarb ooze/chalk of unit III occurs within a 25-meter uncored interval. Minor amounts of forams, micarb, and volcanic glass are present in this unit. A number of thin ash beds, plus a few black scattered ashy spots, also occur in places. Some of the glass grains are up to 1 mm in diameter. Radiolaria and sponge spicules amounting to 25 and 20 percent, respectively, are significant constituents of this unit. It has a lower average percentage of carbonate (70%) than the overlying unit and has only 0.1 percent organic carbon (Figure 4). A thin chert band occurs at the top of Core 12, and chert fragments are found in the core catcher.

Unit IV

The unit consists of 39 meters of massive light orange micarb-rich nanno chalk with thin chert bands. Micarb grains in this unit are colorless, of various shapes (needle-like, irregular, elliptical, etc.), and show a high birefringence. Average carbonate percentage of the unit is 75 percent (Figure 4). Many intervals are foram, spicule-, rad-, or volcanic glass-bearing. At its base, the unit is in contact with basalt. For a distance of 155 cm above this

contact, the sediments have a pale yellowish-green color and exhibit lamination. Some of the laminae dip 5 to 15 degrees. There is no visible effect of the underlying basalt on the sediments. Bulk X-ray results from Core 17 show 97 percent calcite and 3 percent clinoptilolite. The less than 2 μ analyses indicate that cristobalite is a common constituent. Electron microscope studies (see Matter, this volume) reveal the presence of cristobalite spherules. These may constitute up to 30 percent of the sediment near the bottom of Core 18.

Unit V

This lithologic unit is represented by basalt flows and by two thin interbedded sediment layers. At least 6 flows can be distinguished, based on chilled margins which are tan in color. The chilled zones consist of an outer layer of unaltered brown glass (3-4 cm thick) grading downwards into variolitic basalt (~5 cm) consisting of spherules of plagioclase and pyroxene. The flows are represented by 7.4 meters of basalt recovered from a 21.5-meter cored interval encountered in Cores 18 to 21. Vesiculation is not conspicuous with the average vesicles less than 300 microns. Several zones of glass on the top surfaces of flows and sparse vesiculation indicate extrusion of the lava on the ocean floor. The basalt is broken by fractures and veins. Some of the veins are filled with calcite and a reddish-brown mineral. The basalt is fine grained with intergranular texture. Plagioclase (~An₅₀) laths form an interlocking framework filled in by anhedral clinopyroxene and glass. The clinopyroxene is colorless to brown and sometimes forms skeletal crystals. Thin sections from the top of the basalt indicate a fine-grained variolitic texture with phenocrysts of plagioclase and amygdules filled with chlorite. A thin section from 18, CC reveals fine-grained amygdaloidal basalt with intersertal texture. Rough modal analyses indicate plagioclase ~60 percent, clinopyroxene ~20 to 30 percent, glass ~20 percent, opaques <2 percent, and minor amounts of pyrite. The rock is extremely fresh and no secondary alteration could be detected.

Calcareous sediments occur in a 4-cm and a 0.5-cm bed in Cores 19 and 20, respectively. The 4-cm bed consists mainly of micarb with some chlorite, forams, and nannos. The color varies from grayish brown to grayish green. In Core 20, the green calcareous sediment contains almost 100 percent authigenic carbonate. The lowest sediment bed is 15 meters above the base of the deepest penetrated basalt,

which suggests additional deeper sediment layers are probably not present.

Due to limited space, the tables of grain size, carbon carbonate, X-ray, and pH and salinity are presented with the data of other sites in Appendices I, II, III, and IV, respectively, at the end of the volume.

BIOSTRATIGRAPHY

Foraminifera

The downhole distribution of planktonic foraminiferal zones is indicated in Figure 5.

Pleistocene faunas are present at Site 220 in Cores 1 and 2, but the highly fragmented state of many of the tests indicates moderate to high levels of solution. Well-preserved faunas and displaced benthic species suggest turbidites at two horizons (Samples 1-2, 69-71 cm and 2, CC), and minor Eocene and Pliocene constituents in sediments of the former signify that some reworking has occurred. Sample 3, CC contained a small fauna including several Late Miocene or Early Pliocene species as well as *Globorotalia truncatulinoides* and was probably contaminated during drilling. Planktonic species are also rare in Cores 4 and 5 where the relative abundance of deep-water (lower bathyal to abyssal) benthic forms suggests intense solution of the plankton. The few species in these cores are generally of undifferentiated Middle Miocene to Early Pliocene age, but very rare specimens of *Turborotalia acostaensis* in Sample 4-5, 70-72 cm indicate an age no older than Late Miocene (N.16) for this horizon. Rare restricted Middle Miocene species are present in the very small faunas from Core 5, but these may have been reworked like those observed in the Late Miocene at Site 219.

Foraminifera are somewhat more abundant in Core 6 through Core 9, Section 4, but the faunas are relatively nondiverse and zonal determination is difficult. Throughout these samples, *Turborotalia siakensis* and *T. opima nana* are present while *T. opima opima* is absent; an age of P.22 (Late Oligocene) is indicated. This last is present in Sample 9, CC with relatively nondiagnostic taxa representative of the P.20-P.21 (Middle to Late Oligocene) interval. Planktonic foraminifera in Core 10 are rare and of probable P.20 age, and are absent in Core 11.

Core 12 contains a well-developed and well-preserved fauna of Middle Eocene (P.11) age, with common *Morozovella aragonensis aragonensis*. The highest occurrence of *Hantkenina mexicana aragonensis* is located in Sample 13-1, 70-72 cm, which is taken as the top of Zone P.10. The P.10/P.9 boundary is poorly defined but is here recognized at the top of the range of *Acarinina soldadoensis angulosa* (Sample 15-3, 70-72 cm). Sample 16-2, 68-70 cm contains the latest occurrence of *Morozovella aragonensis caucasica* and is taken as the highest sample referred to P.8; specimens of typically younger species (*Globigerinatheka senni*, *G. subconglobata* s.s.) are probably due, in this sample, to contamination during drilling immediately prior to its collection. Faunas of this age (Early Eocene) persist as low as Sample 19-2, 45-47 cm, which contains a well-preserved P.8 assemblage in sediments intercalated in the basalts.

Nannofossils

Hole 220 was drilled in sediments ranging in age from Pleistocene to Early Eocene and underlain by basalt with

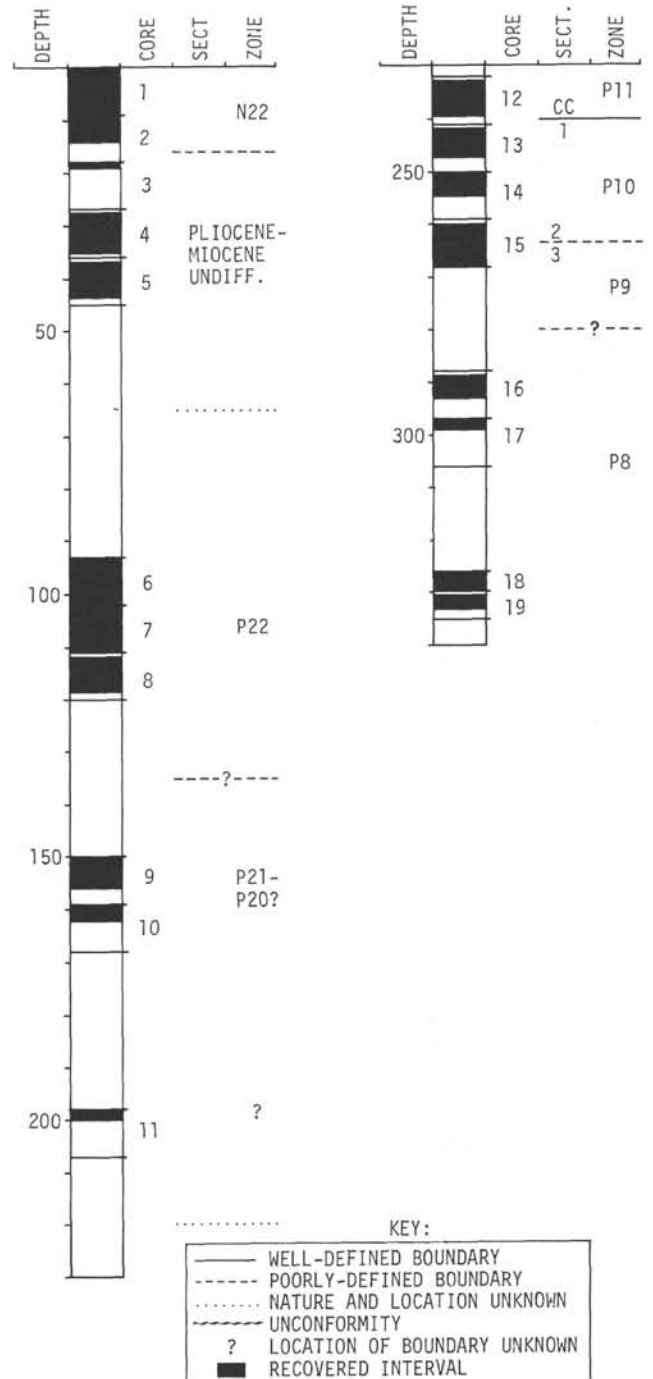


Figure 5. Foraminiferal zonation, Site 220, depth in meters.

intercalated sediment. A bathyal environment occurs throughout most of the stratigraphic sequence. Floods of nannofossils represent a highly developed floral occurrence in Tertiary sediments. Many nannofossil zones could be identified, and all evidence suggests that a nearly complete stratigraphic section is present at Site 220.

The short Pleistocene section present in Core 1 and Sample 2-3, 65-66 cm is characterized by *Gephyrocapsa caribbeanica* (Boudreaux and Hay, 1969), *Pseudoemiliania lacunosa*, *Coccolithus daronicoides*, and *Gephyrocapsa oceanica*. The *Discoaster brouweri* Zone (Boudreaux and Hay, 1969, and Hay et al., 1967) appears in the Late

Pliocene interval in Sample 2, CC. The *Reticulofenestra pseudoumbilica* Zone is present in Sample 3, CC. The extinction level of *Discoaster quinquaramus* is used to determine the Late Miocene/Early Pliocene boundary as seen in Sample 4-4, 65-66 cm. The late Middle Miocene interval appears in Cores 4 and 5 and is recognized by the presence of *Discoaster hamatus* and *Catinaster coalitus*.

The Middle and Early Miocene intervals were not continuously cored. Nannofossil ooze is present in the Late Oligocene interval and is also present in the older section below down to, or near, the cherty section in the Lower Eocene.

The Oligocene/Miocene boundary was not cored at Site 220. *Sphenolithus ciperoensis* is the diagnostic nannofossil used to establish the Late Oligocene interval as seen in Sample 6-1, 66-67 cm. The Middle Oligocene sequence is characterized by the presence of *Sphenolithus distentus* and *Sphenolithus predistentus* as found in Sample 9-1, 65-66 cm. Lower Oligocene sediments were not recovered at this site.

The Late Eocene is present in Sample 11-1, 65-66 cm as verified by the presence of *Discoaster barbadiensis* and *Discoaster saipanensis*. *Sphenolithus spiniger* Bukry and *Sphenolithus obtusus* Bukry are found in the Middle Eocene in Cores 12 and 13. *Chiasmolithus grandis* is present in Sample 12-2, 65-66 cm also suggesting a Middle Eocene age for this interval. The early Middle Eocene appears in Sample 15-4, 65-66 cm with the presence of *Discoaster subloboensis*. The *Discoaster lodoensis* Zone marks the late Early Eocene boundary in Sample 16-2, 87-88 cm. The Early Eocene interval extends from Sample 16-2, 87-88 cm down to Core 18. Core 18 contains specimens of *Discoaster lodoensis*.

Chert is present near the bottom of Core 18. Basalt was penetrated immediately below the chert section. A thin green chloritic sediment layer between two basalt flows in Sample 19-2, 45-46 cm contains rare nannofossils of questionable age.

Radiolaria

At Site 220, Radiolaria are rare or absent in Cores 1 through 5 (0 to 45 m below the sea floor). The hole was then drilled from 45 to 93 meters. A good radiolarian assemblage was first recovered from Core 6 and belongs to the *Calocyclus virginis* Zone (Upper Oligocene according to nannofossil data).

Abundant and well-preserved radiolarian assemblages are found in Cores 6 to 8 (93 to 120 m), but the Radiolaria in Cores 9 and 10 show signs of solution. In addition to polycystine Radiolaria, numerous Orosphaerids are present in Cores 7 to 9.

Cores 7 and 8 belong to the *Dorcadospyrus ateuchus* Zone (Oligocene); Cores 9 and 10, to the *Theocyrtis tuberosa* Zone (Oligocene). In this interval, the assignment of zones is based on the work of Riedel and Sanfilippo (1971). The zonation of Moore (1971) could not be applied satisfactorily to this part of the stratigraphic column. Certain species, e.g., *Theocyrtis annosa* and *Lychnocanoma elongata* (Vinassa), which are stratigraphically important in Pacific Ocean sediments, are absent from Site 220 material.

Core 11 is in the *Thyrsoyrtis bromia* Zone (Upper Eocene according to nannofossil data) and Cores 12 through 14, Section 3, all lie within the *Thyrsoyrtis*

miacantha Zone (Middle Eocene). The *Theocampe mongolfieri* Zone (Middle Eocene) extends from Sample 14-CC to Core 16, Section 2. Below the latter, the assemblage is quite diverse, but not well preserved, and may be said only to be Lower Eocene.

Biostratigraphic Summary

With respect to the nannofossils, Site 220 contains a rich floral assemblage which ranges, in an almost complete stratigraphic section, from Pleistocene to Lower Eocene (0 to 330 m), however, most of the Upper Miocene appears to be missing. Even within the chert and basalt intervals of the hole, sufficient nannofossils may be found in intercalated sediments for reliable age determinations. Such an abundance of nannofossils is indicative of favorable preservation factors in the sedimentary environment at Site 220 since Early Eocene time.

In contrast, the planktonic foraminiferal faunas are generally impoverished and partially dissolved throughout the sequence representing Pleistocene to Oligocene time (i.e., 0 to 180 m below the sea floor). Benthonics are rare and represent lower to middle bathyal depths. Below 232 meters, however, a relatively well developed planktonic fauna was observed and persists down the hole to the top of the basalt. This sequence is apparently complete, representing each of the Paleogene foraminiferal zones down to Zone P.8.

Radiolaria are rare or absent in the top 45 meters of Hole 220. They are abundant and generally well preserved from 93 to 306 meters and represent a fairly complete section from the Upper Oligocene to the Lower Eocene.

The stratigraphic sequence at Site 220 may be divided, on its biogenous content, into 4 units:

- 1) 0 to 45 meters—nannofossils only (Pleistocene to Middle Miocene).
- 2) 93 to 207 meters—nannofossils and Radiolaria (Upper Oligocene to Upper Eocene).
- 3) 232 to 306 meters—nannofossils, Radiolaria, and foraminifera (Upper Eocene to Lower Eocene).
- 4) 306 to 330 meters—poor fossils (nannofossils, Radiolaria, foraminifera) in chert and basalt.

Sedimentation rates are nearly constant for the upper 2 units but increased noticeably during the Middle Eocene when all three of the fossil groups treated are present in quantity. There is no faunal evidence for marked changes in water depth during the Tertiary; a change in the depth of the lysocline may explain some of the observed faunal variations. If McElhinny's (1970) plate reconstructions are correct, the area of Site 220 has been in tropical latitudes in post-Miocene time. By comparisons with present-day patterns of oceanic circulation at various latitudes, one would then expect reasonably high radiolarian productivity in the upper 45 meters of Site 220. Since this is not the case, as shown by the recovered cores, it would appear that one must postulate either a poorly developed circulation and/or changes in ocean chemistry.

Sedimentation Rate

Sedimentation rates are generally variable (Figure 6). Lower Eocene sediments (290 to 332 m) accumulated at a rate greater than 40 m/m.y. This value decreased to 19 m/m.y. during the Middle Eocene (234 to 290 m), and further to 6 m/m.y. in the Late Eocene through Middle

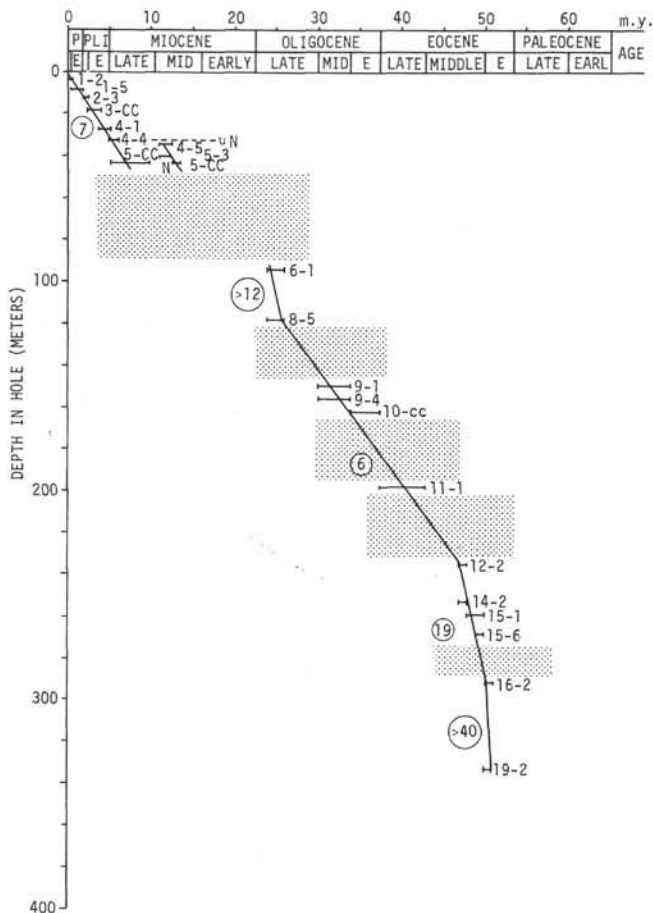


Figure 6. Sedimentation rate curve, Site 220. Plotted bars are those sufficient to control slopes of lines. Stippled pattern represents some uncored intervals. See Chapter 2, Explanatory Notes, for explanation of age ranges and other symbols.

Oligocene. Paleontologic control is inadequate for the calculation of a rate for the Late Oligocene, but it was at least 12 m/m.y.

Two determinations are possible for the interval between 34 and 43 meters. If the nannofossil determinations for the ages of these samples are correct, the sedimentation rate may be as low as 2 and as high as 20 m/m.y., and an unconformity must be present between Sections 4 and 5 of Core 4. The rate derived for this interval from foraminiferal ages is the same as that for the remainder of the Late Neogene (0 to 31 m), 7 m/m.y. In either case, the presence or absence of an unconformity in the drilled interval between Cores 5 and 6 (43 to 93 m) cannot be determined.

GEOCHEMISTRY

The distribution of trace elements in sediments retrieved from Site 220 is somewhat similar to that found in the sediments of Site 219 (Figure 7).

Magnesium, titanium, chromium, nickel, iron, and vanadium seem to be enriched in the upper 50 meters of sediment at this site. Smear slide data indicate the presence of clay-sized detrital material in this interval. No detrital material was found in the lower sediment interval (50 to 330 m). Thus, this enrichment of trace metals in the upper 50 meters may be related to the detrital material.

Manganese in the sediments shows a somewhat different distribution pattern; it seems to be enriched in both upper and lower parts of the section examined. More X-ray mineralogical data are needed to explain its behavior at this site.

PHYSICAL PROPERTIES

Sediment Density, Porosity, and Water Content

Sediment density shows a general increase with depth from the sea bed to about 150 meters. Low GRAPE density values in Core 1 (ca. 1.25 g/cc) along with porosity values in excess of 80 percent and water content approaching 50 percent reflect the soupy nature of this first core. The more soupy intervals have a similar effect at other depths in the hole. Undisturbed Core 4, with densities around 1.51 g/cc, marks the top of a gradient, related to increasing compaction with depth, which extends down to Core 9 (density of about 1.67 g/cc. Voids and slurred sections in Cores 10 and 11 probably account for the low values and fluctuations in density encountered there. However, a major change can be noted in Cores 12 to 14, where GRAPE density values vary between 1.42 and 1.53 g/cc. The syringe and bulk section density values do not appear to be lowered as markedly over this interval. It is suggested that this feature can be correlated with the lithologic importance here of Radiolaria and sponge spicules. This intermittent occurrence of hydrous opaline silica is probably responsible for the general lowering and fluctuation in values as measured by the GRAPE device.

Cores 16 and 17 show increased fluctuation in density due to their alternating chalk and ooze lithology, prominent chert layers and voids. The low values in Core 17 are due to its broken-up nature. The highest GRAPE values (greater than 2.0 g/cc) in Cores 12, 16, and 17 appear to correlate with the major chert layers.

An interesting sequence of GRAPE density changes occurs in Core 18, which incorporates the sediment/oceanic basement contact. The core starts at the top with chert layering within chalk and is followed by compact chalk with no chert down to the basement contact. The average density over this interval is 1.85 g/cc, but the chert layers at the top fall within a 2.0 to 2.5 g/cc range. Next, a major step-up occurs in the density plot at 239 meters, where chalk of density 1.85 g/cc overlies basalt.

Compressional Wave Velocity

Velocity generally increases through the sediment column from about 1.48 km/sec to 1.91 km/sec. Variations from this trend are slight except for high values of up to 4.0 km/sec in the chert layers of Cores 16 and 17.

The sediment/basalt contact is outlined by a change to values around 4.5 km/sec.

Specific Acoustic Impedance

In general, this parameter parallels the sonic velocity graph, but major density fluctuations have a corresponding effect on acoustic impedance as in the lower values in Core 13.

The graph effectively pinpoints the major reflectors by relatively high values in the chert layers, which become important below 290 meters, and in the basalt below 329 meters. The occurrence of these reflectors within 40 meters

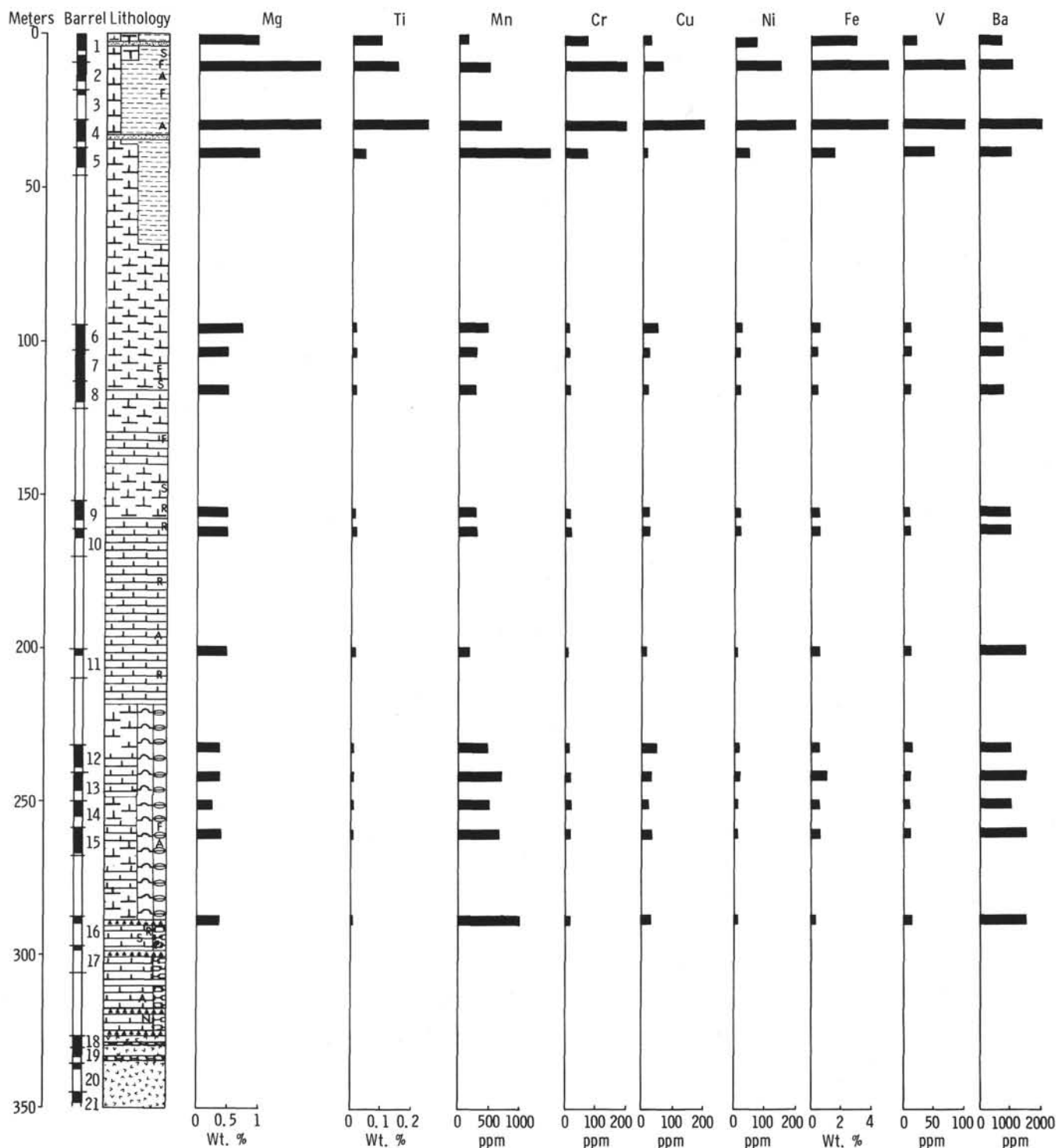


Figure 7. Chemistry of the sediments from Site 220.

of one another makes it probable that the major reflector on the geophysical records is the chert masking the effect of the basement below.

CORRELATION OF REFLECTION PROFILES AND LITHOLOGIES

At Site 220, the general uniformity of the lithology of most of the cored section and the several drilled intervals made it difficult to correlate the observed reflections with

significant lithology changes. The site lay over a rather transparent layer which was upfaulted or folded immediately east of the site to form a low flat-topped hill (Figure 8). At the foot of the hill, well-stratified sediments are seen to onlap the transparent layer. At the base of this layer, there is a strong conformable reflection which is very diffuse, being spread over about 0.2 seconds. This reflector is so strong that on occasion multiples representing paths with additional reflection at the sea bed or sea surface are

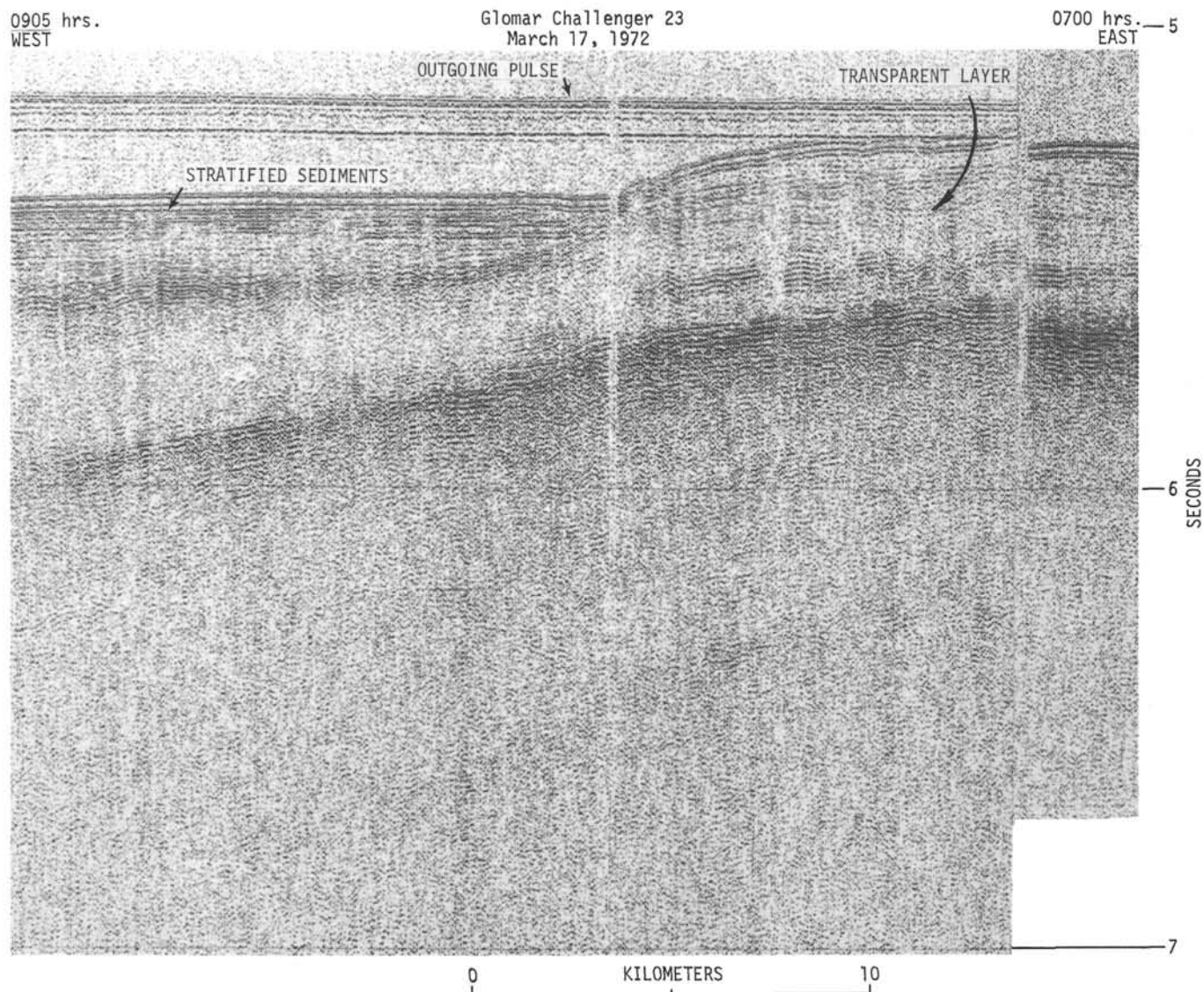


Figure 8. A seismic reflection profile obtained by Glomar Challenger across the west edge of the hill about 10 km northwest of Site 220. The profile shows the general relationship of the various reflectors cored at the site.

seen. Just above this reflection there is a weaker discontinuous reflection.

On the airgun profile obtained on departure over the beacon, reflections were picked out at 0.05, 0.21, and 0.32 seconds of two-way travel time below the sea bed (Figure 9). The 0.05 second reflection represents the base of the stratified layer and probably corresponds to the base of the cored sequence of occasional foraminiferal sand and brown clay nannofossil ooze, although this could not be confirmed because of a gap in coring. The reflection at 0.21 seconds seems to be due to the gradual ooze-to-chalk transition, and the reflection at 0.32 seconds is certainly due to the chert which, although it first appears at 233 meters, is not fully developed until 290 meters. The mean velocity to the chert is therefore 1.81 km/sec. These data are summarized in Figure 10.

PALEOMAGNETIC MEASUREMENTS

A total of 31 samples were taken for preliminary paleomagnetic study. The 14 sediment samples are

principally laminated chinks of Middle and Early Eocene age. Eight of these samples come from a 1-meter interval within Core 14, Section 3. The remaining 6 samples are representative of a 2.5-meter interval within the chalk facies of Core 18 immediately above the contact with the oceanic basement. The 17 basalt samples are distributed uniformly throughout the recovered length of 7.4 meters of basalt from the 21-meter cored interval. Table 3 gives the results of the remanence measurements on these samples.

Laminated Chalks

The laminated chalk samples have a mean intensity of magnetization of $3.63 \pm 0.87 \times 10^{-6}$ G/cm³, with the highest intensity values restricted to those samples from Core 18.

Assuming no rotation within Core 14, Section 3, then the individual remanence directions can be referred to a common azimuthal orientation. Figure 11 shows the distribution of natural remanent magnetization (NRM) directions for this core section. Apart from 2 samples, the

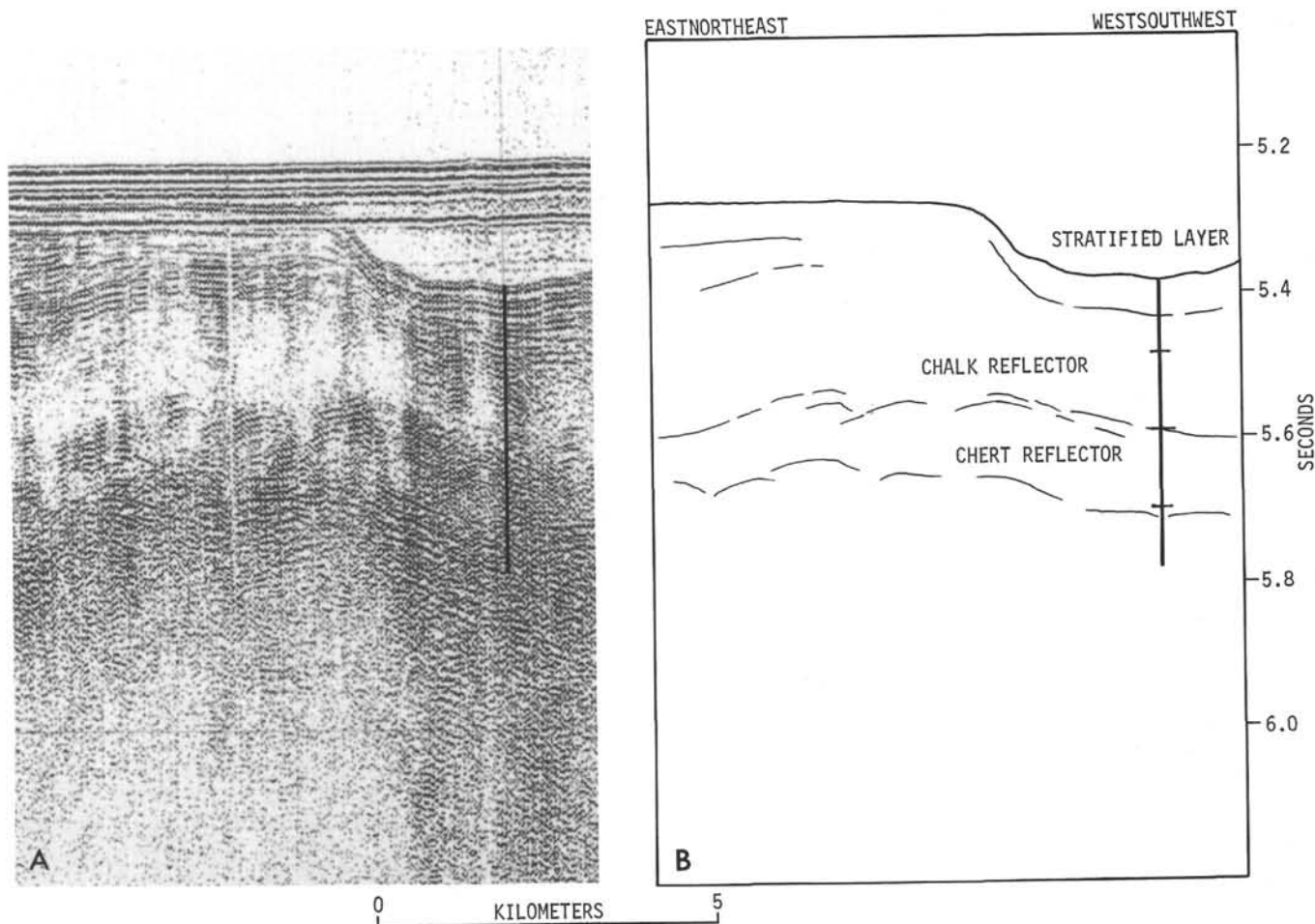


Figure 9. (a). Seismic reflection profile obtained on departure from the site. The ship passed directly over the sea floor acoustic beacon. The approximate penetration of the drill string is shown by the vertical line. The horizontal banding at the top of the profile is due to the outgoing signal from the airguns and is not part of the profile. (b). A line drawing showing the interpretation of Figure 9a used to produce Figure 10. The vertical line has tenth second divisions.

remainder are scattered within one quadrant of the stereogram and have a positive inclination. Fisher's (1953) statistics have been used to calculate a mean direction for this group: D_m (relative) = 35.1° , $I_m = 17.1^\circ$, $K = 13.5$, $a_{95} = 18.9^\circ$, $R = 5.631$, and $n = 6$. On partial demagnetization in a peak field of 50 oersted, there is no reduction in the observed scatter: D_m (relative) = 312.3° , $I_m = 28.4^\circ$, $K = 10.8$, $a_{95} = 21^\circ$, $R = 5.538$, and $n = 6$. It should be noted that this latter mean direction shows a declination change of 83° from that of NRM direction together with an increase in inclination. Some 20 percent of the original NRM intensity remains after demagnetization.

On the whole, the Lower Eocene chalk samples show similar variable behavior. The scatter in inclination is somewhat reduced after partial demagnetization. Sample 18-3, 29 cm was subjected to progressive demagnetization, the results of which are given in Table 4 and the normalized intensity decay curve included on Figure 12. The approximate invariance of the remanent vector during demagnetization to peak field values of 150 oersted suggests some degree of stability.

The respective values for mean absolute inclination of the Middle and Lower Eocene samples after partial demagnetization are $25.7 \pm 3.6^\circ$ and $17.0 \pm 3.4^\circ$. This result is rather anomalous. On the basis of a northward

movement of the Indian plate during Eocene time, a steeper absolute inclination would be expected for the older sediment sequence, not the reverse as indicated by the observed values. A possible explanation for this apparent discrepancy may relate to the fact that in Core 14, Section 3, the visible lamination dips at up to 20° in some of the measured samples. The direction of dip of those laminae can be estimated with respect to the split face of the core from observations on individual samples. If these dips are post-depositional, then the absolute inclination should be corrected for a tilting effect. It can be shown that the application of this correction will shallow the observed mean absolute inclination appreciably, certainly reducing it below the mean value found for Core 18. Notwithstanding this explanation, there remains the possibility that magnetic instability may also account, to some extent, for the discrepancy.

A mean absolute inclination of 22.0 ± 2.7 degrees is given for the combined data after demagnetization.

Basalts

Observed remanent intensities of the basalt samples lie in the range 2.8 to 60×10^{-4} G/cm³ with a mean value of $2.85 \pm 0.38 \times 10^{-3}$ G/cm³.

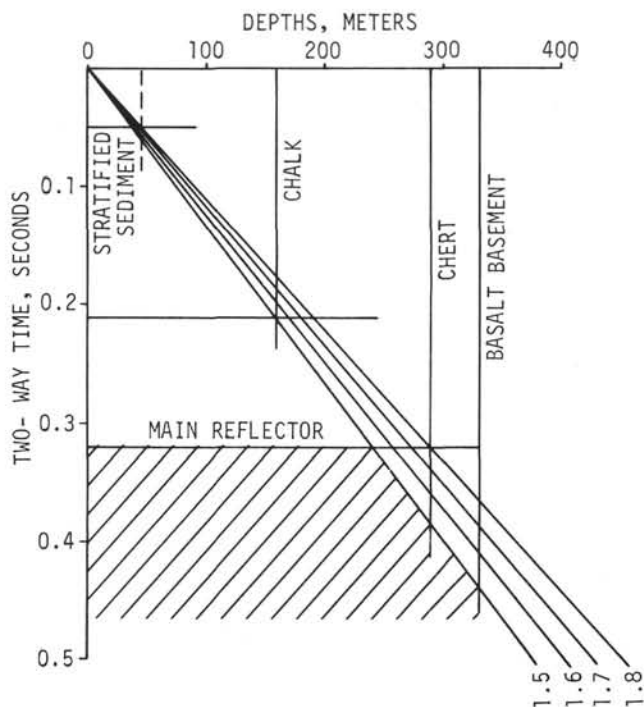


Figure 10. Plot of reflection times beneath Site 220 against the depths of significant changes in lithology found in the cores. Lines are drawn corresponding to mean velocities of 1.5, 1.6, 1.7, and 1.8 km/sec.

Remanence results both before and after partial alternating field (Af) demagnetization are characterized by low and variable inclination values. After demagnetization, the mean absolute inclination value is $12.0 \pm 1.5^\circ$, which is significantly lower than that of the overlying Eocene sediments. Three samples, 18-4, 62 cm, 19-2, 2 cm, and 10-2, 132 cm, exhibit negative inclinations, but absence of known relative azimuthal orientation with respect to adjacent samples precludes the recognition of a true polarity reversal on the basis of a 180° declination change. Further, since the observations here on possible reversals are based on single isolated samples they are of limited value. The occurrence of a reversal within a single flow is not a common observation.

Sample 20-1, 52 cm was progressively demagnetized in fields of increasing strength up to 600 oersted. The results of this procedure are given in Table 4, and Figure 12 shows the normalized intensity decay curve. Figure 13 illustrates the migration pattern of the remanent vector during this progressive demagnetization. The decay on intensity is fairly rapid, less than 15 percent of the NRM intensity remains after demagnetization at peak field values in excess of 150 oersted. Up to this field value, the remanent vector shows only a limited change in its orientation. More erratic behavior typifies its orientation after demagnetization in higher fields. This is thought to indicate instability for this sample.

With the exception of Sample 19-1, 102 cm, the sampled basalts show a similar rapid intensity decrease on partial demagnetization to that exhibited by the pilot sample described above. For the majority of samples, less than 20 percent of the NRM intensity remains. Such behavior is in

marked contrast to that of stable terrestrial basalts, which retain a far greater percentage of their magnetization on demagnetization in low fields of comparable strength as shown by the basalts studied from hole EM 7, Mohole project, by Cox and Doell (1962).

Such observations appear to indicate that the fractured basalts sampled at this site may well have acquired an appreciable viscous magnetization component since the time of their original extrusion. This could account for the low mean absolute inclination value.

DISCUSSION AND CONCLUSIONS

Geological Setting

This site is located in the Arabian Sea approximately 740 km west-southwest of the southern tip of India at a subsea depth of 4036 meters. Site 219 lies 320 km to the northeast, and Site 221 is situated 280 km to the northwest. The bathymetric map by R. L. Fisher (unpublished) and Plate 1 in the pocket at the back of the volume show Site 220 as being situated on a broad deep platform several thousand meters below the Laccadive-Chagos Ridge to the east. Directly to the west of the platform lies the rough topography of the Carlsberg Ridge. There, extensive transform faulting has created long high north-northeast ridges separated by deep troughs. Although the ridges are barren, the troughs have a fill of transparent sediments. The sea floor at Site 220 lies 500 to 1000 meters above the level of this fill.

Previous track charts in the area, plus the *Glomar Challenger* sea floor and seismic profiling records, indicate that much of the platform surface at this site is covered by a layer of ponded sediments. Although in proximity to the nearby Arabian Abyssal Plain, the two areas are apparently of differing topographic elevations. They are separated in part by the above mentioned transform fault ridge topography. Furthermore, the southernmost margin of the Arabian Abyssal Plain, as seen near Site 221, is more than 100 km north and 600 meters deeper than the abyssal plain under discussion here.

The latter apparently is bounded on the south by the same topography which marks its western margin. Ponding to the east is provided by the Laccadive-Chagos Ridge. No obvious topographic feature marks its northern termination, and, perhaps, an interbedding of sediments from the two abyssal plains occurs there. The ponded surface drilled at this site, which is outlined roughly by the 4000 meter contour, appears to be about 400 to 500 km long and 50 to 100 km wide.

The cover of stratified sediments on the abyssal plain is thin, reaching a maximum thickness of 250 to 300 meters, 30 km west of Site 220. Beneath the stratified layer is a 250- to 300-meter-thick sequence of transparent sediments which uniformly mantles the undulating basaltic basement. However, locally the transparent interval protrudes above the level of the ponded surface resulting in the development of low irregular hill topography. Site 220 was drilled where the stratified sediments onlap such a hill, and it is, therefore, situated at the edge of the ponded surface.

TABLE 3
Summary of Magnetic Data, Site 220

Sample (Interval in cm)	NRM			Af Demagnetization			
	Intensity (G/cm ³)	Relative Declination (degrees)	Inclination (degrees)	Peak Field (oersted)	Intensity (G/cm ³)	Relative Declination (degrees)	Inclination (degrees)
Sediments							
14-3, 10	1.2 × 10 ⁻⁶	121.8	20.6	50	8.0 × 10 ⁻⁷	60.4	29.9
14-3, 21	2.3 × 10 ⁻⁶	15.8	16.4	50	9.6 × 10 ⁻⁷	296.6	17.3
14-3, 31	2.0 × 10 ⁻⁶	11.4	3.2	50	9.6 × 10 ⁻⁷	287.7	31.5
14-3, 41	2.1 × 10 ⁻⁶	26.7	17.3	50	6.4 × 10 ⁻⁷	281.2	46.5
14-3, 51	1.8 × 10 ⁻⁶	43.2	11.2	50	7.9 × 10 ⁻⁷	344.2	18.3
14-3, 61	2.1 × 10 ⁻⁶	64.5	30.9	50	7.7 × 10 ⁻⁷	326.7	21.8
14-3, 71	1.5 × 10 ⁻⁶	53.9	18.6	50	8.9 × 10 ⁻⁷	327.6	23.8
14-3, 90	9.6 × 10 ⁻⁷	198.2	25.2	50	7.6 × 10 ⁻⁷	68.2	16.3
18-2, 22	4.3 × 10 ⁻⁶	353.7	-23.1	50	1.5 × 10 ⁻⁶	88.6	24.2
18-2, 145	8.4 × 10 ⁻⁶	97.4	10.2	50	5.3 × 10 ⁻⁶	112.0	14.9
18-3, 29	1.0 × 10 ⁻⁵	69.8	2.1	50	4.7 × 10 ⁻⁶	71.7	- 5.2
18-3, 59	2.8 × 10 ⁻⁶	72.3	21.7	50	5.8 × 10 ⁻⁷	23.8	28.6
18-3, 89	9.9 × 10 ⁻⁶	320.4	24.5	50	8.4 × 10 ⁻⁶	317.8	13.7
18-3-119	1.4 × 10 ⁻⁶	348.8	79.9	50	2.5 × 10 ⁻⁶	283.9	15.4
Basalts							
18-4, 7	6.1 × 10 ⁻³	316.0	15.7	100	2.1 × 10 ⁻³	322.4	21.2
18-4, 62	1.4 × 10 ⁻³	90.8	-16.7	100	2.3 × 10 ⁻⁴	122.8	- 9.4
18-4, 109	1.2 × 10 ⁻³	317.0	9.0	100	1.9 × 10 ⁻⁴	294.5	9.3
19-1, 58	3.7 × 10 ⁻³	107.2	10.6	100	7.0 × 10 ⁻⁴	124.7	9.0
19-1, 102	2.8 × 10 ⁻⁴	97.1	16.8	100	1.9 × 10 ⁻⁴	180.3	3.8
19-2, 2	7.6 × 10 ⁻⁴	306.1	- 8.0	100	1.5 × 10 ⁻⁴	281.9	- 7.3
19-2, 42	3.3 × 10 ⁻³	120.7	14.9	100	3.7 × 10 ⁻⁴	121.9	10.2
19-2, 82	2.3 × 10 ⁻³	19.8	9.5	100	5.1 × 10 ⁻⁴	22.7	10.5
19-2, 132	4.5 × 10 ⁻³	44.4	-22.4	100	8.5 × 10 ⁻⁴	44.7	-20.1
20-1, 9	3.9 × 10 ⁻³	101.2	9.4	100	5.8 × 10 ⁻⁴	114.1	7.1
20-1, 52	2.1 × 10 ⁻³	26.4	7.0	100	7.6 × 10 ⁻⁴	42.5	7.1
21-1, 22	1.8 × 10 ⁻³	327.1	26.1	100	2.4 × 10 ⁻⁴	296.1	14.0
21-1, 72	3.6 × 10 ⁻³	253.2	23.6	100	4.9 × 10 ⁻⁴	252.3	21.3
21-1, 122	2.1 × 10 ⁻³	181.6	37.2	100	3.0 × 10 ⁻⁴	175.4	15.4
21-2, 25	3.1 × 10 ⁻³	323.0	19.7	100	1.1 × 10 ⁻³	311.9	20.9
21-2, 72	4.9 × 10 ⁻³	86.0	10.9	100	1.8 × 10 ⁻³	91.2	14.1
21-2, 125	3.4 × 10 ⁻³	52.3	5.1	100	3.9 × 10 ⁻⁴	58.2	2.5

The Stratigraphic Column

A 329 meter discontinuously cored sediment interval plus 21 meters of basalt, containing two thin sediment layers, were penetrated. A total of 21 cores recovered 93.5 meters of sediment and 7.4 meters of basalt. The sediments record almost continuous deposition of pelagic calcareous nannofossils from Early Eocene to Pleistocene time. These fossils are mixed with large amounts of other pelagic products such as brown clay and siliceous fossils which, together with varying amounts of micarb particles and the presence or absence of chert, serves to divide the column into four lithologic units. Minor amounts of foraminifera, volcanic glass, clinoptilolite, cristobalite, and tridymite are

revealed by smear slide studies and X-ray mineralogy. A fifth lithologic unit encompasses the basaltic interval at the bottom of the hole.

The topmost lithologic unit encountered in Cores 1 to 5 is marked by its brown color, by thin foraminiferal sands, and by an almost equal admixture of clay and nannofossils. These admixtures vary to form brown detrital clay nanno ooze and brown nanno detrital clay sediments. The foraminiferal sands, which vary in thickness, represent turbidity current deposits generated in the shallower waters of the Laccadive-Chagos islands. Similar sands were noted in a piston core taken from the same ponded surface by von Stackelberg (1972). They occur throughout unit I, which encompasses Late Pleistocene through Late or Middle

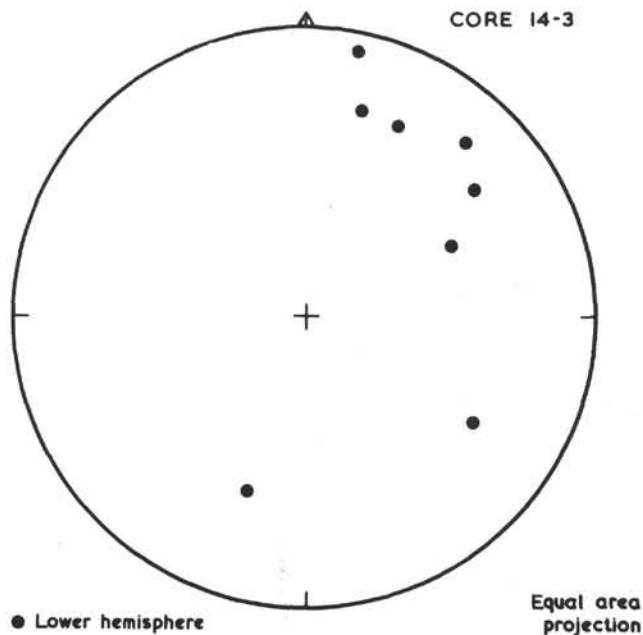


Figure 11. Distribution of remanence directions of Core 14, Section 3 plotted with respect to an arbitrary zero.

Miocene time.² Only the most obvious sands are indicated on the core summary forms. Foraminifera are also locally prominent in the oozes (up to 15% in Core 1). They exhibit moderate to high solution activity.

Because its contact with the underlying lithologic unit was not cored, the thickness (ca. 69 meters) and age of unit I are not precisely defined. Its sediments appear to include the stratified interval seen on the seismic profiler records.

A profound compositional change occurs between units I and II which manifests itself in many ways. Megascopically, the color alters from brown to white, which under the microscope reflects a decrease in clay minerals and an increase in nannofossils. The X-ray bulk mineralogy also records an abrupt carbonate increase which is similarly monitored by the carbon-carbonate studies. Finally, the spectrochemical data records a sudden decrease of magnesium, titanium, chromium, nickel, iron, and vanadium.

The sediments of unit II, as well as those of units III and IV, are dominated by nannofossils plus prominent admixtures of radiolarians and sponge spicules. Variations in the proportions of these fossil groups, plus progressive downhole changes in induration and diagenetic alteration, characterize these sediments. Some of the changes and variations serve to define the three units.

² At Site 220, a dichotomy of opinion exists regarding the extent of the Late Miocene interval in unit I. Shipboard nannofossil studies suggest a thin Late Miocene interval with an unconformity in Core 4. The core forms reflect this viewpoint. Foraminiferal studies plus shore-based nannofossil studies indicate a thick Late Miocene interval is present extending beyond Sample 5, CC. Because an unconformity in this interval, which would represent deposition on an abyssal plain, is unlikely, interpretations in this writeup reflect the latter viewpoint. The hole summary form reflects both viewpoints.

TABLE 4
Af Demagnetization Results, Site 220

Sample	Peak Field (oersted)	Intensity (G/cm ³)	Relative Declination (degrees)	Inclination (degrees)
18-3, 29 cm	NRM	1.0 × 10 ⁻⁵	69.8	2.1
	25	8.1 × 10 ⁻⁶	77.5	1.4
	50	4.7 × 10 ⁻⁶	71.7	-5.2
	75	3.6 × 10 ⁻⁶	78.7	-6.3
	100	3.5 × 10 ⁻⁶	61.6	-4.4
	150	2.7 × 10 ⁻⁶	67.2	-8.6
	200	2.1 × 10 ⁻⁶	52.0	-63.5
20-1, 52 cm	NRM	2.1 × 10 ⁻³	26.4	7.0
	50	1.6 × 10 ⁻³	34.4	11.3
	100	7.6 × 10 ⁻⁴	42.5	7.1
	150	2.5 × 10 ⁻⁴	25.0	2.8
	225	3.0 × 10 ⁻⁴	73.5	-26.5
	300	7.6 × 10 ⁻⁵	56.8	-30.6
	375	8.5 × 10 ⁻⁵	303.3	-0.5
	450	1.7 × 10 ⁻⁴	77.9	-16.3
	525	2.4 × 10 ⁻⁴	297.1	43.3
	600	1.3 × 10 ⁻⁴	202.2	-64.3

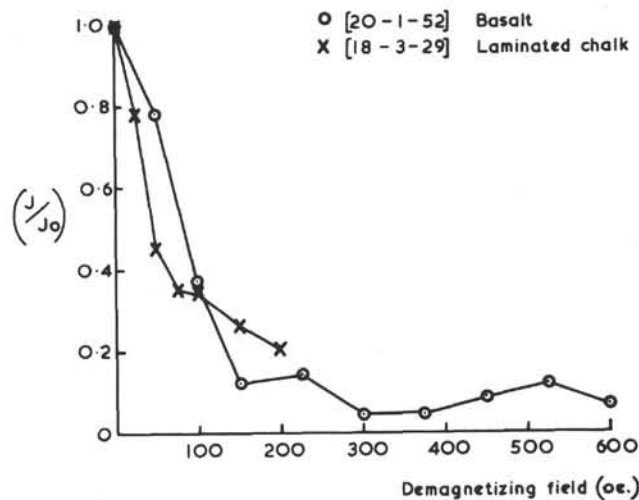
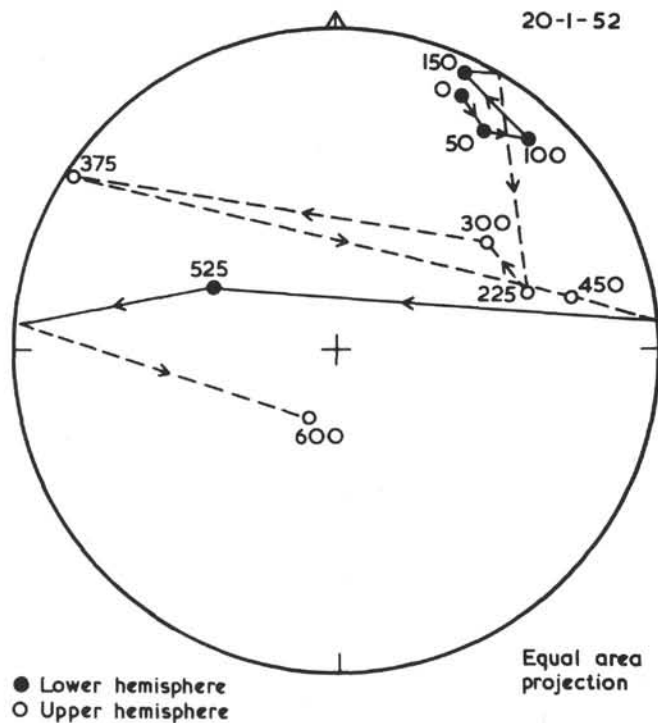


Figure 12. Normalized intensity decay curves.

The nannofossil oozes which mark unit II gradually become more consolidated, developing an alternating chalk-ooze facies in the Upper Oligocene sediments beginning at a downhole depth of 114 meters. Then, beginning at 288 meters, the Lower Eocene nannofossil oozes have completely altered to a chalk facies. Also, starting at the top of the Upper Eocene strata, carbonate particles of unknown origin, termed "micarb," begin to appear at a depth of 232 meters. These progressively increase with depth. On the basis of electron-microscope work, most of these particles are probably an alteration product of nannofossils.

Regarding siliceous organisms, radiolarians first make a noticeable appearance in the Middle Oligocene rocks of unit II. However, it is not until Middle Eocene strata are encountered that they, along with sponge spicules, make a significant contribution to the sediments, an aspect which serves to define unit III. The large amounts of opaline silica in the sediments may be responsible for a GRAPE density decrease at this depth.



● Lower hemisphere
○ Upper hemisphere
Numbers indicate peak field in oersted.
Figure 13. Behavior of basalt Sample 20-1, 52 cm during stepwise demagnetization.

Siliceous tests in the Lower Eocene strata have undergone significant alterations to produce silicified chalk and chert layers (one thin chert layer does occur in Middle Eocene sediments). This facies marks the beginning of unit IV. Additional evidence of sediment alteration is provided by the X-ray mineralogy studies which reveal significant cristobalite and minor amounts of tridymite and clinoptilolite. Electron microscope work by A. Matter reveals that the cristobalite is present as small spherules.

In units II to IV, foraminifera are present only in small amounts and then as an impoverished and intensely dissolved assemblage. Near the bottom of the stratigraphic column in the Eocene oozes of unit IV, and in the intercalated sediment beds in the basalt, the foraminifera are again well preserved. The latter change in preservation probably reflects a shallow depositional depth relative to the calcium carbonate compensation depth (CCD).

The 7.5 meters of basalt recovered in this hole contain several individual flows, each marked by a chilled zone at its top. Compositionally, the rock appears to be derived from a tholeiitic melt and to be similar to deep ocean basalts. Sparse vesiculation and the formation of glass at the top surface of the flows indicate a deep-water and extrusive origin, respectively. The lack of a chilled zone in the basal sediments also argues for an extrusive origin.

Within the basalt there are two thin sediment layers. The upper one, which occurs 2 meters below the top of the basalt, is a 4-cm-thick limestone bed. The other, a 0.5-cm-thick calcareous chalk layer, is found 7 meters below the upper basalt surface. Only a trace of nondiagnostic nanofossils in a matrix of calcareous particles was noted in the lower thinner sediment layer.

However, a scanning electron microscope (SEM) examination shows the presence mostly of highly altered nanofossils in the upper sediment layer.

Much micarb and a trace of foraminifera are also present. Conflicting paleontologic data in this layer indicate a Late Paleocene age on the basis of nanofossils and Early Eocene on the basis of foraminifera. In spite of more nanofossils being present, the foraminifera show better preservation and their age designation for the sediments, which corresponds to that of the sediments directly above the basalt, was accepted. Although the two sediment intervals could represent xenoliths incorporated in a basaltic extrusion, their uniform thickness across the core, plus a horizontal bedding attitude, suggests that they are thin sediment layers buried by subsequent flows.

Aspects of Sea Floor Spreading and Crustal Age

An age of 51 m.y. has been established for the oldest sediments found at Site 220. Whether this age truly reflects the age of the underlying oceanic crust is difficult to determine. One problem is the conflicting ages for the sediment intercalated in the basalt outlined in the preceding paragraph. Another is the deep chert reflector in this region which masks the small-scale abyssal hill topography in the underlying basalt. This prevents an evaluation as to whether Site 220 was situated on an abyssal hill or in a trough area which in turn bears on whether sedimentation began immediately after the flow of basalt ceased. Consequently, the 51 m.y. must be accepted as a minimal age (although a true age would probably be only a few million years more).

One, therefore, must reconcile an age of 51 m.y. at Site 220 with a basement age of 47 m.y. at Site 221, a region which is 160 km north of Site 220. On the basis of a 2.5 cm/yr spreading rate calculated by Whitmarsh (Chapter 14), the crust directly west of Site 220 at the longitude of Site 221 would be 10 million years younger than at the former site. This necessitates the presence of one or more transform faults separating the two sites. The presence of such faults can easily be inferred from the elongate north-northeast ridges noted on the topographic maps of this area.

Depositional History

Site 220 for much of its depositional history appears to have experienced the sinking which typifies a normal ocean crust moving away from a spreading ridge crest. Perturbations in the expected sediment sequence late in the depositional history seem related to possible structural movement and changes in the CCD.

Formation of normal igneous oceanic crust at Site 220 ceased in Early Eocene time. The presence of two thin sediment layers between basalt flows suggests that short periods of sediment accumulation were interspersed during the last phase of basalt extrusion. Deposition of nanofossil oozes was accompanied by large amounts of radiolarians and sponge spicules. The presence of the siliceous tests suggests that the site was either in an equatorial belt of high productivity which, as Lisitzin (1972) shows, is presently centered just south of the equator, or it was in a coastal

upwelling area. The analysis of paleomagnetic data (Whitmarsh et al., this volume) indicates that Site 220 was at approximately 10°S latitude in Early Eocene time. However, paleogeographic constructions suggest a well-developed equatorial current system was absent and, therefore, coastal upwelling more likely accounts for the siliceous sediments.

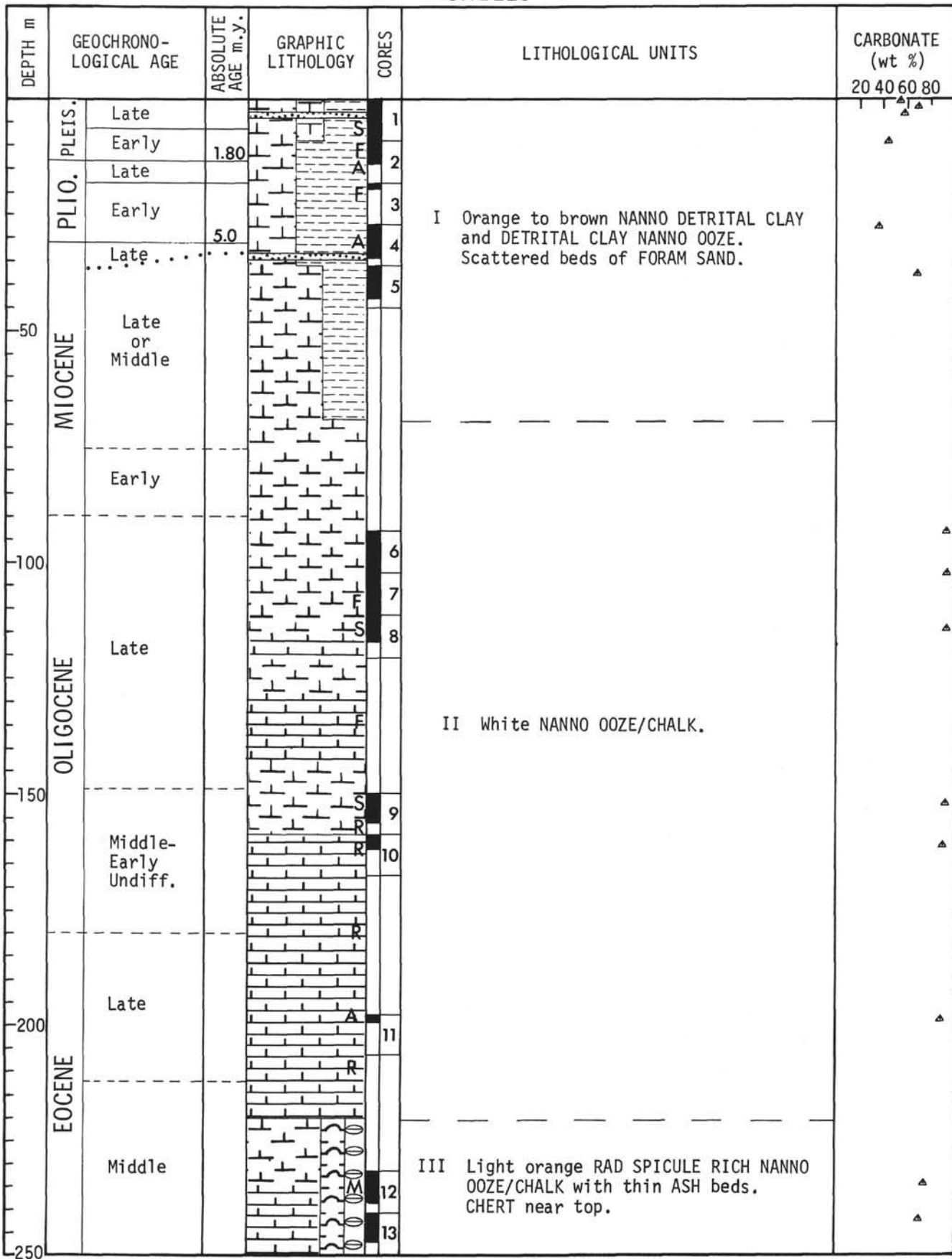
The combination of being situated in a region of productive surface waters and on a shallow crestal ridge resulted in a high initial rate of sediment accumulation. By Late Eocene time, the high surface productivity at Site 220 had apparently ceased. This, in conjunction with its migration into ever-increasing water depths down the ridge flank, resulted in a decreasing rate of accumulation of white nannoplankton ooze. The rate which dwindled to 6 m/m.y. suddenly increased in Late Oligocene time. This increase may reflect structural elevation of the site, possibly due to renewed sea floor spreading from the Carlsberg Ridge in the Oligocene after the hiatus postulated by McKenzie and Sclater (1971).

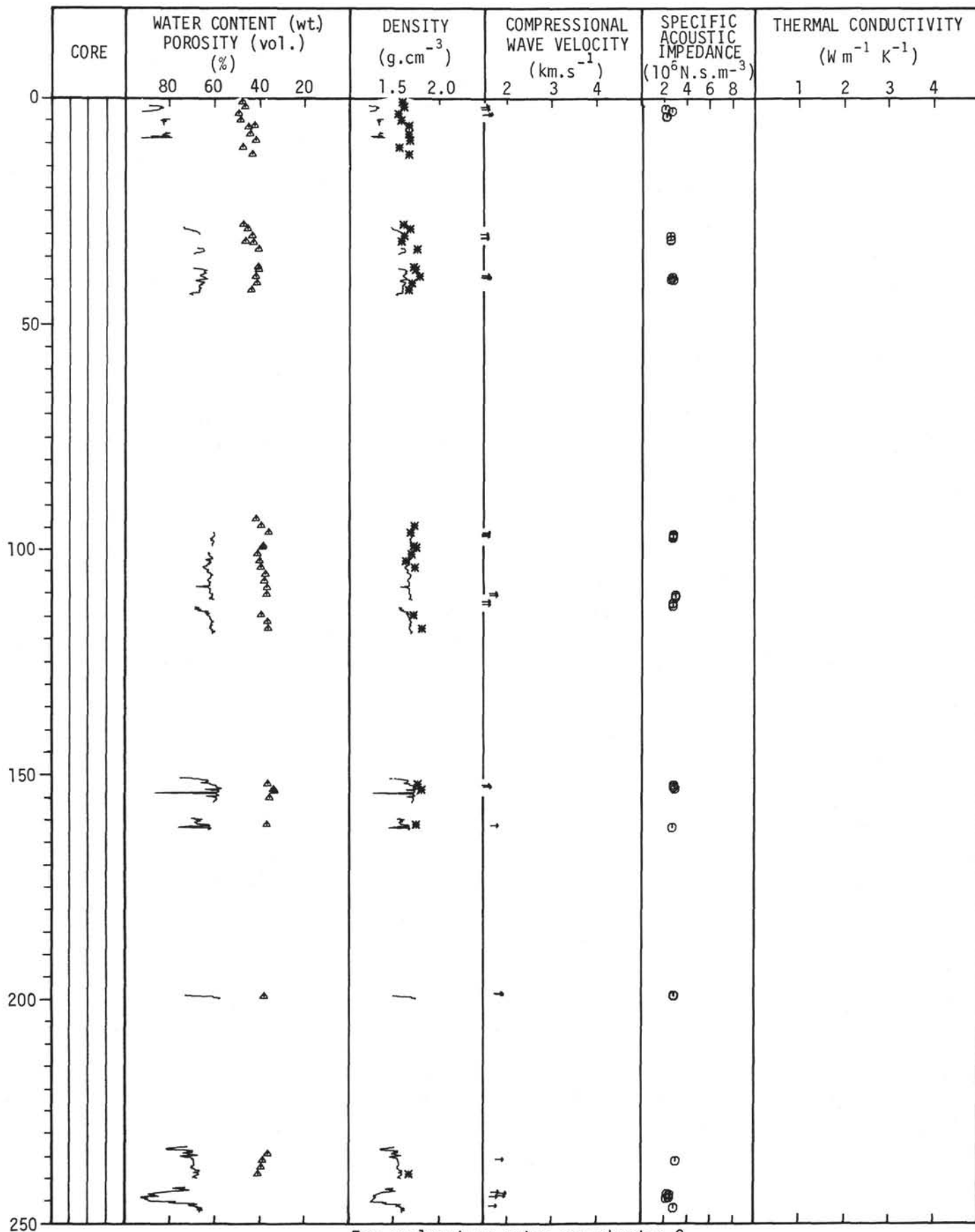
The deposition of almost pure nannofossil ooze was accompanied by a trace of clay particles, a few foraminifera, and slightly larger amounts of Radiolaria and sponge spicules. Much of the subsequent depositional history, although hidden in an uncored interval, may largely have been one of the pelagic brown clay deposition. Deposition of this type is more logical (see Weser, Chapter 12) than continuing nanno ooze sedimentation. However, because this interpretation is highly speculative, this uncored interval is represented on the site summary log by interpolating lithologies from underlying and overlying cores.

Deposition to this point had been in the manner of pelagic draping of fine sediments over the undulating basaltic topography. Subsequently, continuous sediment accumulation included some turbidite deposition. Most of these sediments consist of nearly equal proportions of nannofossils and detrital brown clays, the latter compositionally similar to the gray detrital clays found in the shallower region of Site 219. Interbedded in this interval are thin foram sands containing redeposited shallow-water benthic forms, probably derived from the Chagos-Laccadive Ridge. A decrease upward (from the coring break) of the solution levels of the foraminifera suggests a deepening CCD.

REFERENCES

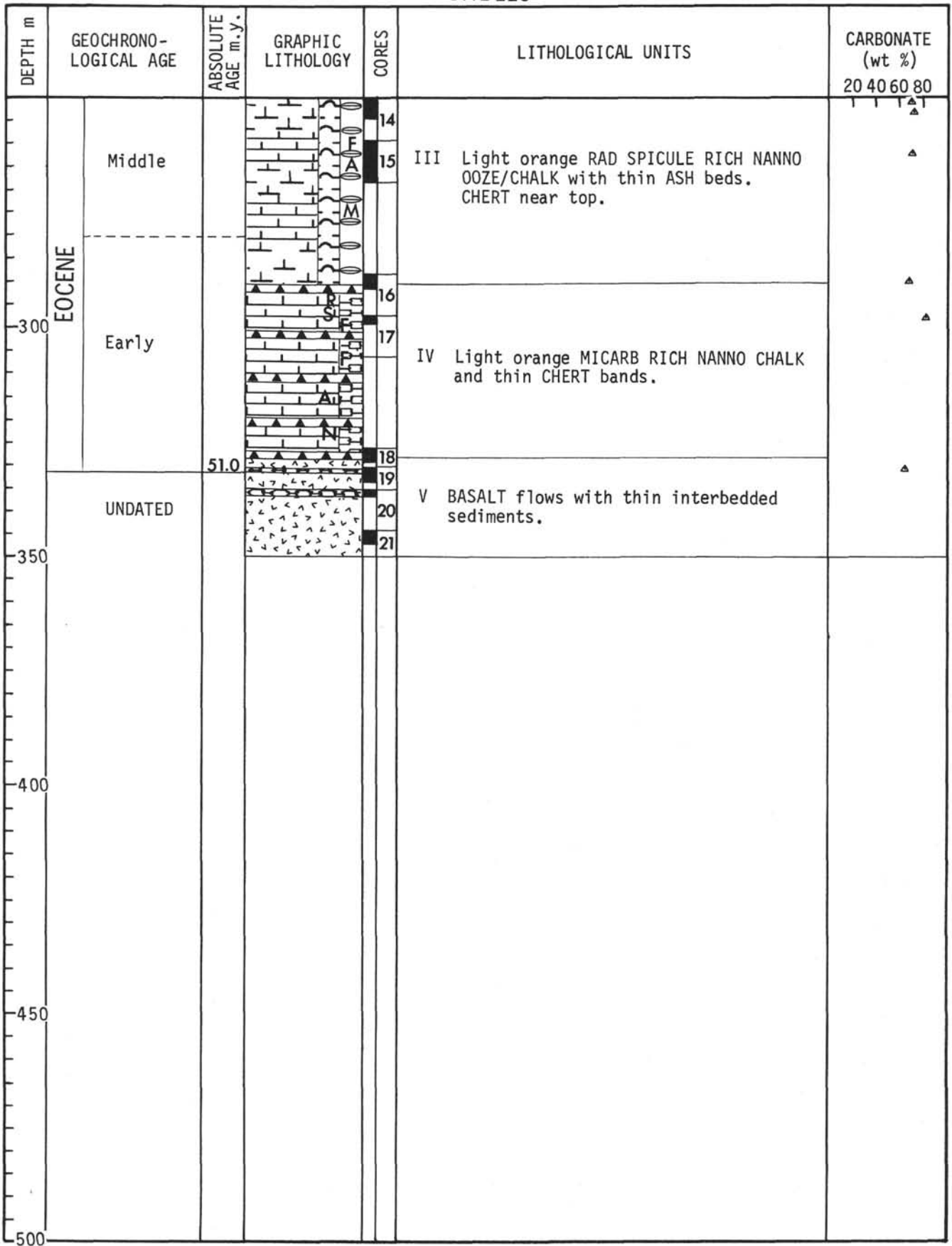
- Boudreaux, J. E. and Hay, W. W., 1969. Calcareous nannoplankton and biostratigraphy of the Late Pliocene-Pleistocene-Recent sediments in the *Submarex* Cores: *Rev. Espanola Micropaleont.*, v. 1, no. 3, p. 249-292.
- Cox, A. and Doell, R. R., 1962. Magnetic properties of the basalt in hole EM 7, Mohole Project: *J. Geophys. Res.*, v. 67, p. 3997.
- Ewing, M., Eittreim, S., Truchan, M., and Ewing, J. I., 1969. Sediment distribution in the Indian Ocean: *Deep Sea Res.*, v. 16, p. 231-248.
- Fisher, R. A., 1953. Dispersion on a sphere: *Roy. Soc., London Proc., Ser. A*, v. 217, p. 295.
- Fisher, R. L., Sclater, J. G., and McKenzie, D. P., 1971. Evolution of the central Indian Ridge, western Indian Ocean: *Geol. Soc. Am. Bull.*, v. 82, p. 553-562.
- Francis, T. J. G. and Shor, G. G., 1966. Seismic refraction measurements in the Northwest Indian Ocean: *J. Geophys. Res.*, v. 71(2), p. 427-449.
- Hay, W. W., Mohler, H. P., Roth, P. H., Schmidt, R. R., and Boudreaux, J. E., 1967. Calcareous nannoplankton zonation of the Cenozoic of the Gulf Coast and Caribbean-Antillean Area and transoceanic correlation; *Gulf Coast Assoc. Geol. Soc. Trans.*, v. 17, p. 428-480.
- Laughton, A. S., Matthews, D. H., and Fisher, R. L., 1971. The structure of the Indian Ocean. *In The Sea, A Maxwell (Ed.): New York (John Wiley & Sons Inc.)*, v. 4(2), p. 543-586.
- Lisitzin, A. P., 1972. Sedimentation in the World Ocean: *Soc. Econ. Paleontol. Min. Spec. Publ. No. 17*, 218 p.
- McElhinny, M. W., 1970. Formation of the Indian Ocean: *Nature*, v. 228, p. 977.
- McKenzie, D. P., and Sclater, J. G., 1971. The evolution of the Indian Ocean since the Late Cretaceous: *Geophys. J. Roy. Astro. Soc.*, v. 25, p. 437-528.
- Moore, T. C., 1971. Radiolaria. *In Tracey, J. I., Jr., Sutton, G. H., et al., Initial Reports of the Deep Sea Drilling Project, Volume 8: Washington (U. S. Government Printing Office)*, p. 727-748.
- Riedel, W. R. and A. Sanfilippo, 1971. Cenozoic Radiolaria from the western tropical Pacific, Leg 7. *In Winterer, E. L., Riedel, W. R., et al., Initial Reports of the Deep Sea Drilling Project, Volume 7: Washington (U. S. Government Printing Office)*, p. 1529-1672.
- von Stackelberg, U. V., 1972. Faziesverteilung in Sedimenten des indisch-pakistanischen Kontinentalrandes (Arabisches Meer): "Meteor." *Forsch-Ergeb. Reihe C*, No. 9, p. 1-73, Berlin, Stuttgart.

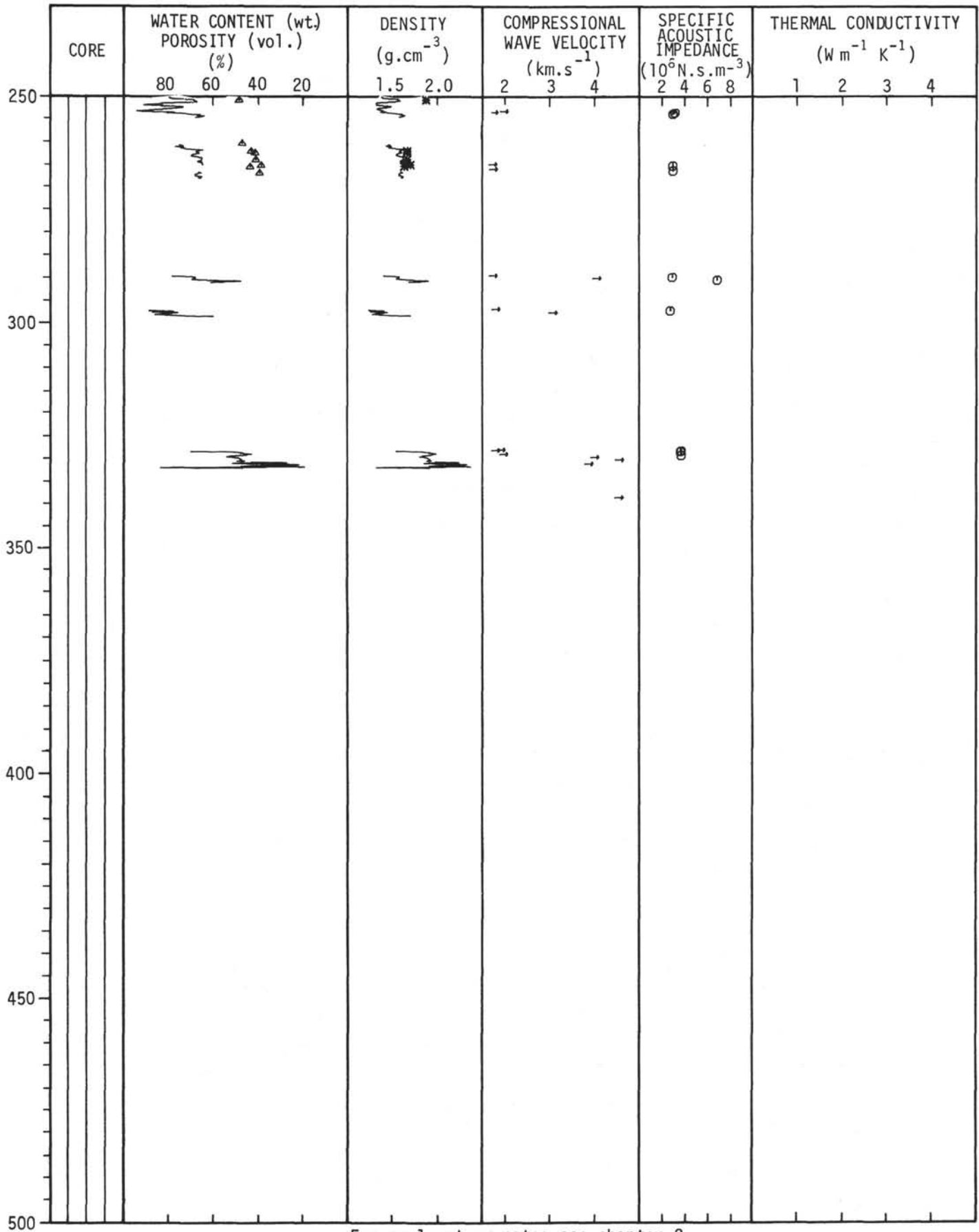




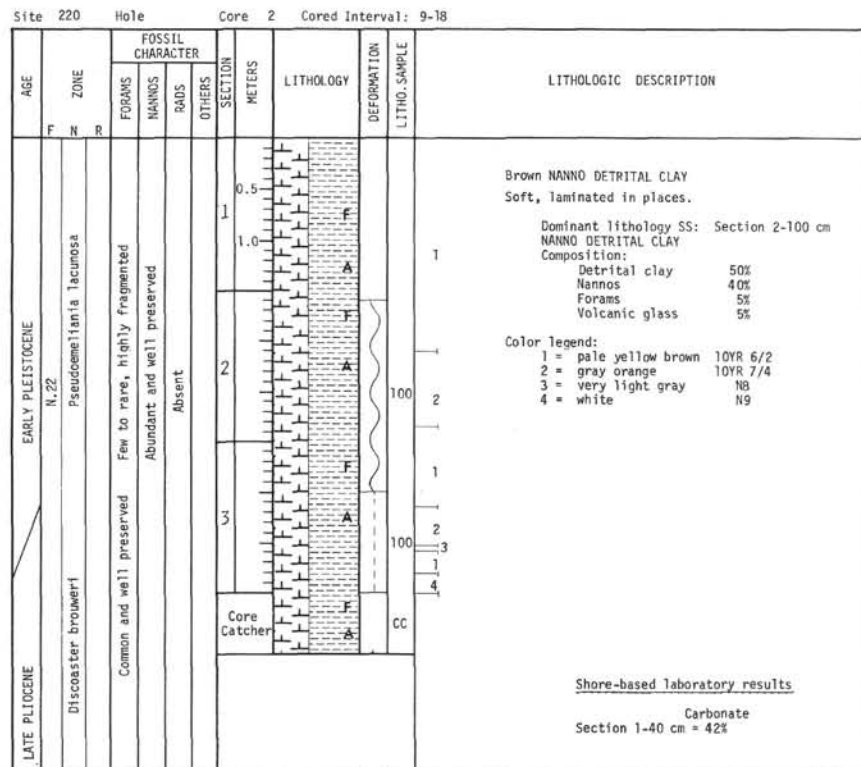
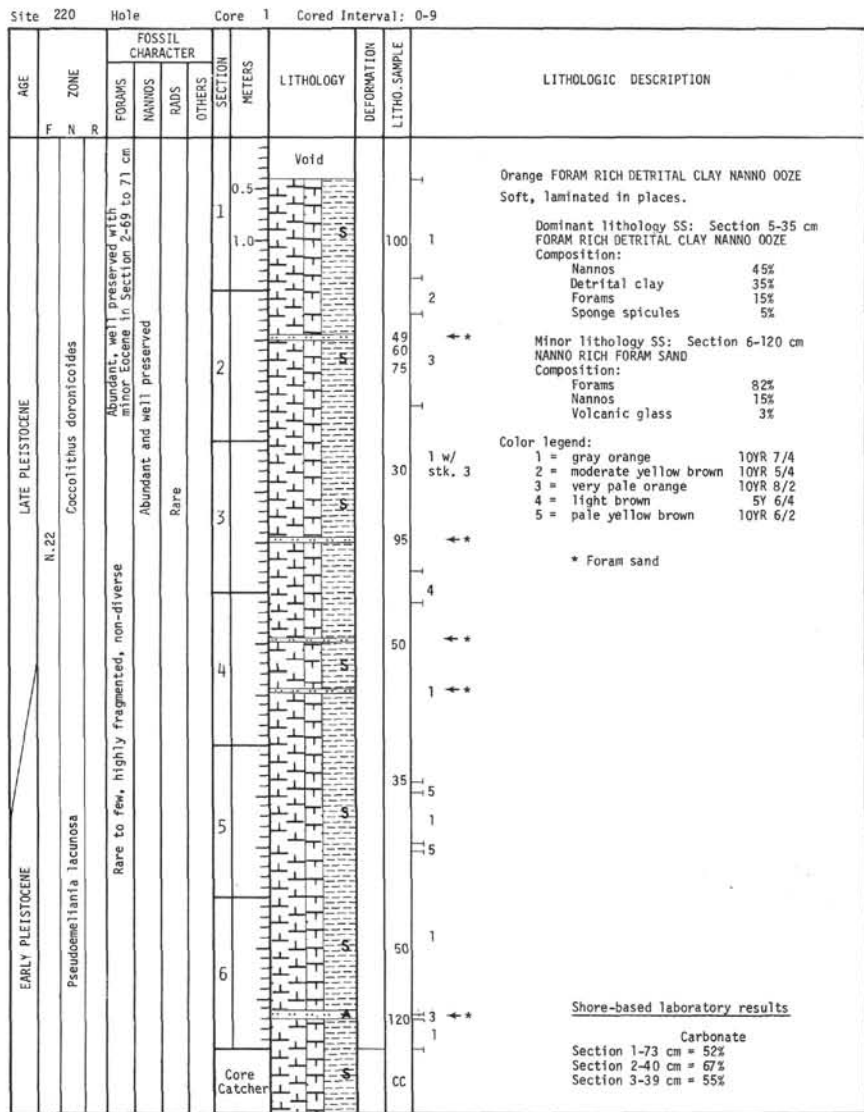
For explanatory notes see chapter 2.

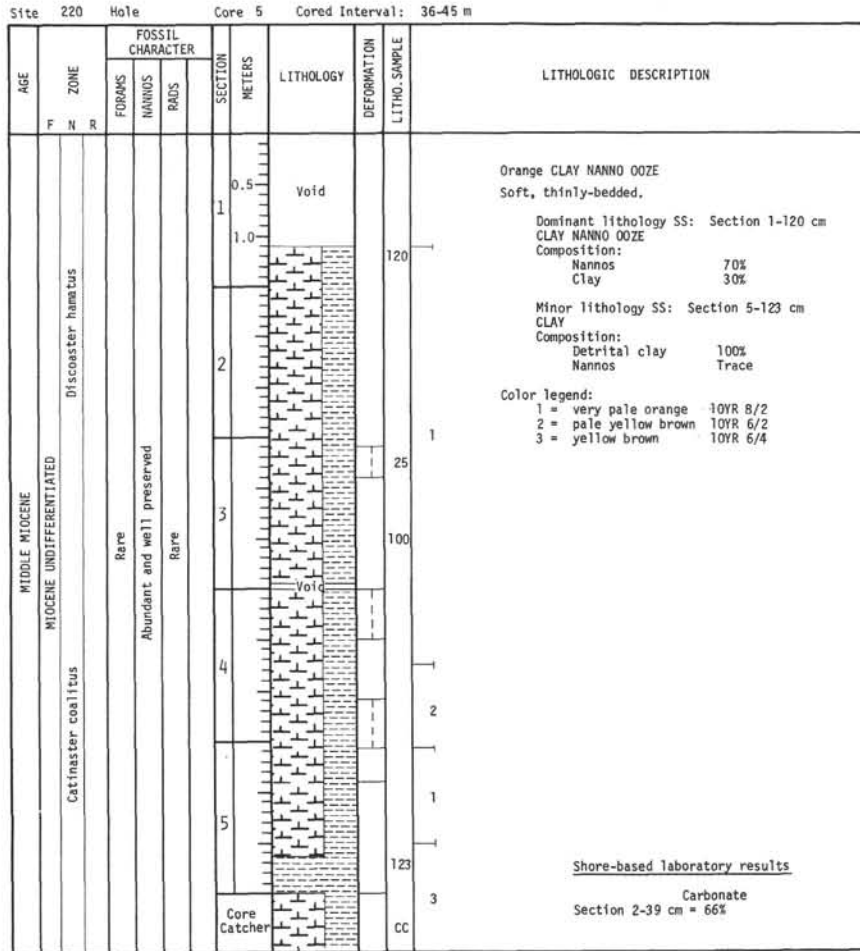
SITE 220



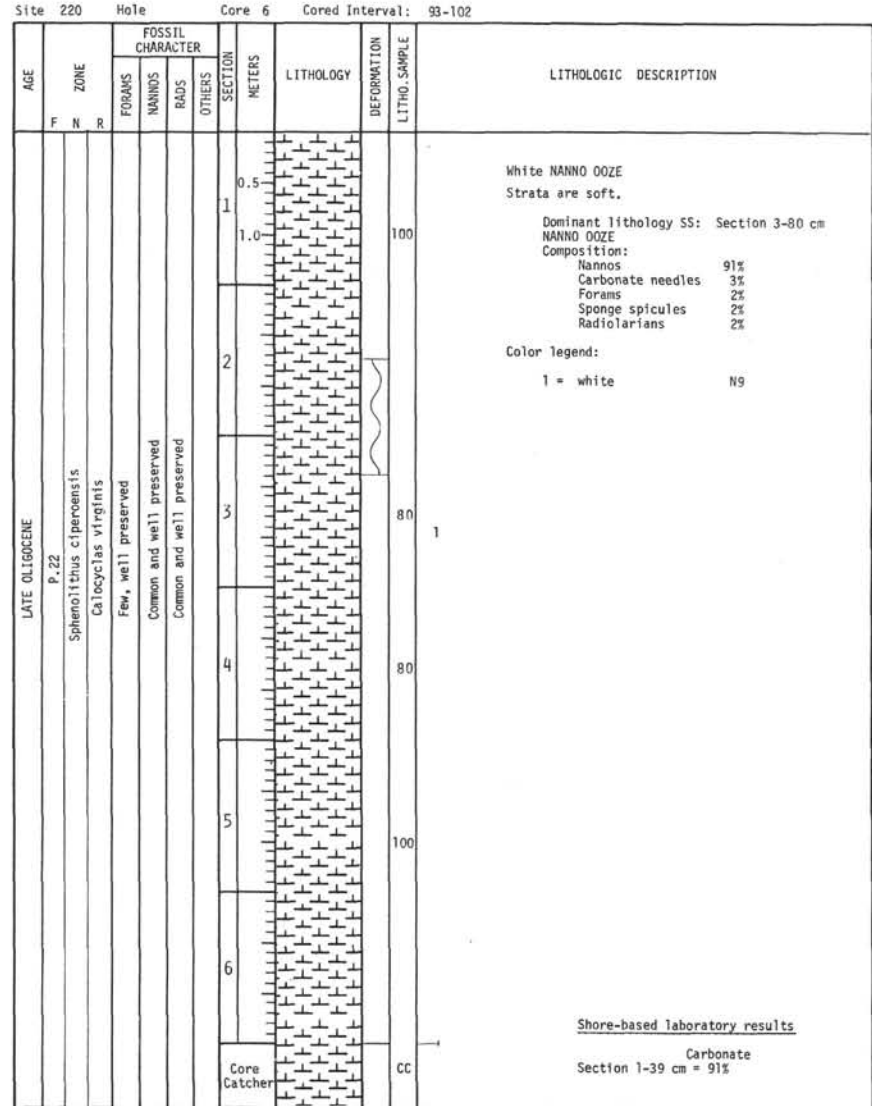


For explanatory notes see chapter 2.





Explanatory notes in chapter 2



Explanatory notes in chapter 2

Site 220 Hole Core 9 Cored Interval: 150-159

AGE	ZONE	FOSSIL CHARACTER				SECTION METERS	LITHOLOGY	DEFORMATION	LITHO. SAMPLE	LITHOLOGIC DESCRIPTION
		FORAMS	NANNOS	RADS	OTHERS					
MIDDLE OLIGOCENE	P.20-21 ?	Sphenolithus praedistans				0.5 1.0		100	White NANNO OOZE and CHALK. Ooze and chalk alternating, well-bedded, soft and hard layers. Dominant lithology SS: Section 1-100 cm NANNO OOZE Composition: Nannos 90% Radiolarians 7% Sponge spicules 3% Color legend: 1 = white N9	
		Theocyrtis tuberosa				2		80		
						3		1		
						4				
						Core Catcher		CC	Shore-based laboratory results Carbonate Section 2-40 cm = 90%	

Site 220 Hole Core 10 Cored Interval: 159-168

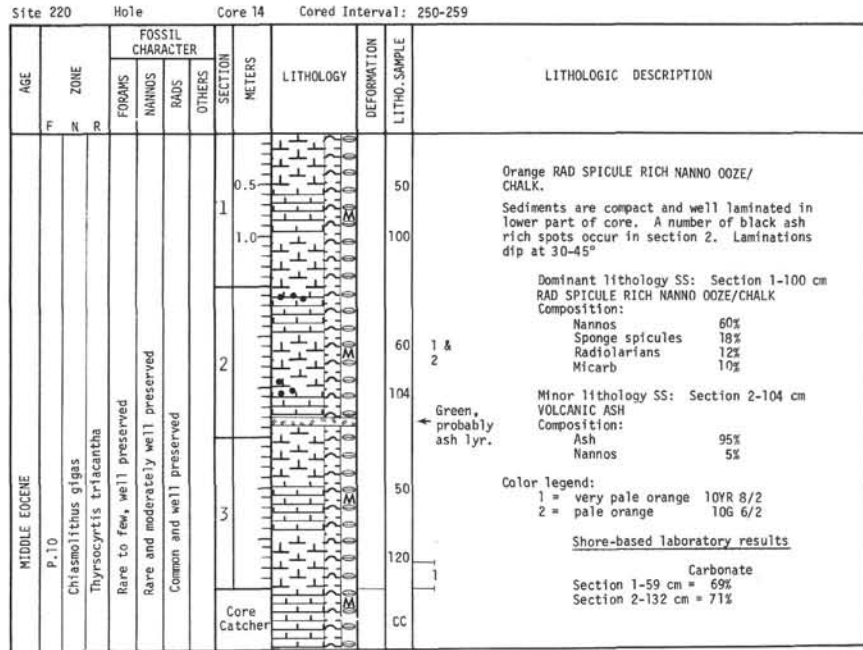
AGE	ZONE	FOSSIL CHARACTER				SECTION METERS	LITHOLOGY	DEFORMATION	LITHO. SAMPLE	LITHOLOGIC DESCRIPTION
		FORAMS	NANNOS	RADS	OTHERS					
MIDDLE OLIGOCENE	P.20-21 ?	Sphenolithus praedistans				0.5 1.0	Void		1	White NANNO CHALK. Homogenous and compact. Dominant lithology SS: Section 2-100 cm NANNO CHALK Composition: Nannos 91% Radiolarians 5% Sponge spicules 2% Forams 2% Color legend: 1 = white N9
		Theocyrtis tuberosa				2		100		
						Core Catcher		CC	Shore-based laboratory results Carbonate Section 2-40 cm = 88%	

Explanatory notes in chapter 2

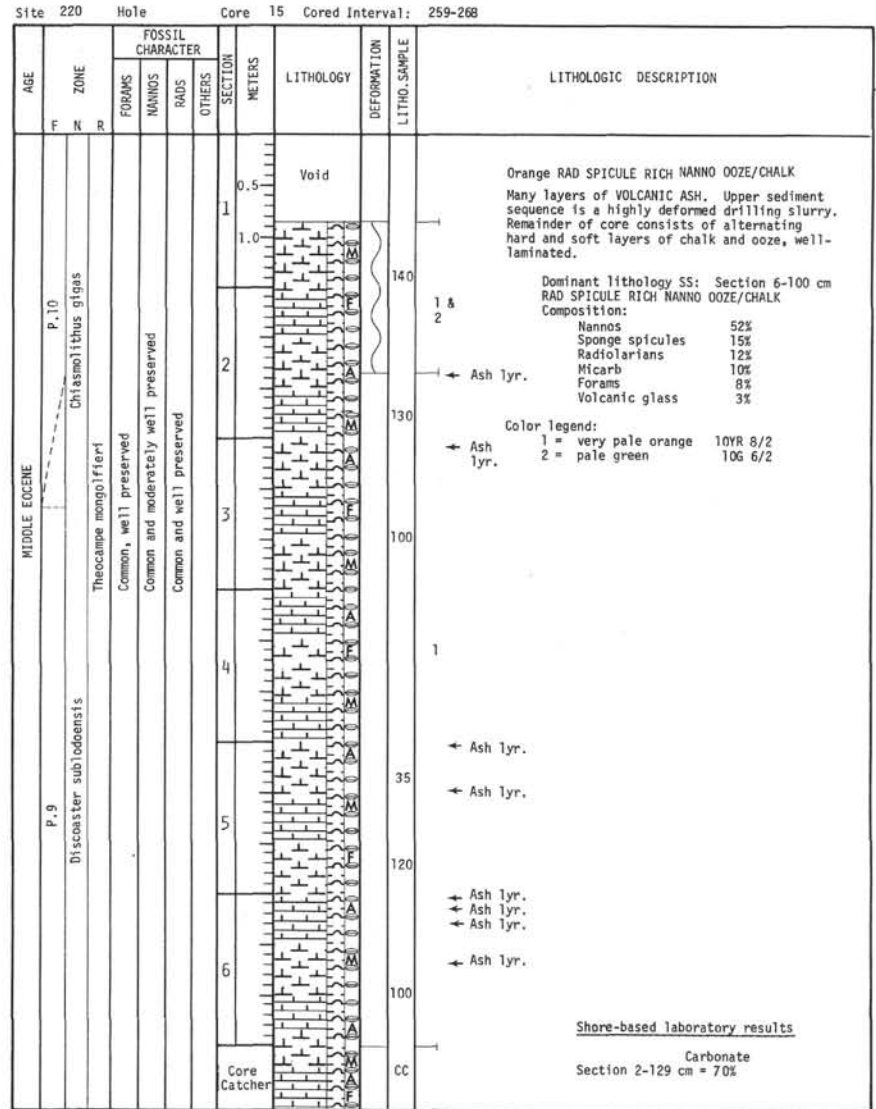
Site 220 Hole Core 11 Cored Interval: 198-207

AGE	ZONE	FOSSIL CHARACTER				SECTION METERS	LITHOLOGY	DEFORMATION	LITHO. SAMPLE	LITHOLOGIC DESCRIPTION
		FORAMS	NANNOS	RADS	OTHERS					
LATE EOCENE		Discoaster barbadensis				0.5 1.0		40 100	1	White NANNO CHALK. Occasionally glass rich, homogenous in texture. Dominant lithology SS: Section 1-100 cm NANNO CHALK Composition: Nannos 95% Radiolarians 5% Sponge spicules Trace Minor lithology SS: Section 1-40 cm VOLCANIC GLASS RICH NANNO CHALK Composition: Nannos 60% Volcanic glass 25% Forams 5% Radiolarians 5% Sponge spicules 5% Color legend: 1 = white N9
		Thyrsocyrtis bromia				Core Catcher		CC		* black grains <u>Shore-based laboratory results</u> Carbonate Section 1-35 cm = 87%

Explanatory notes in chapter 2

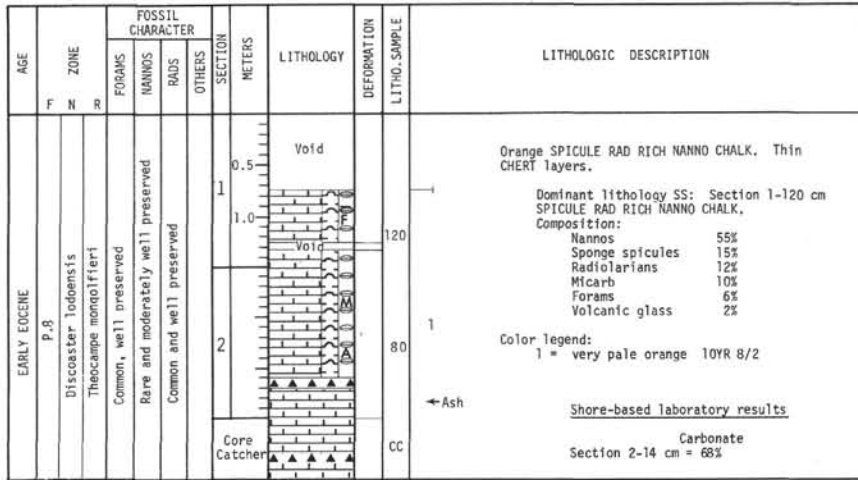


Explanatory notes in chapter 2

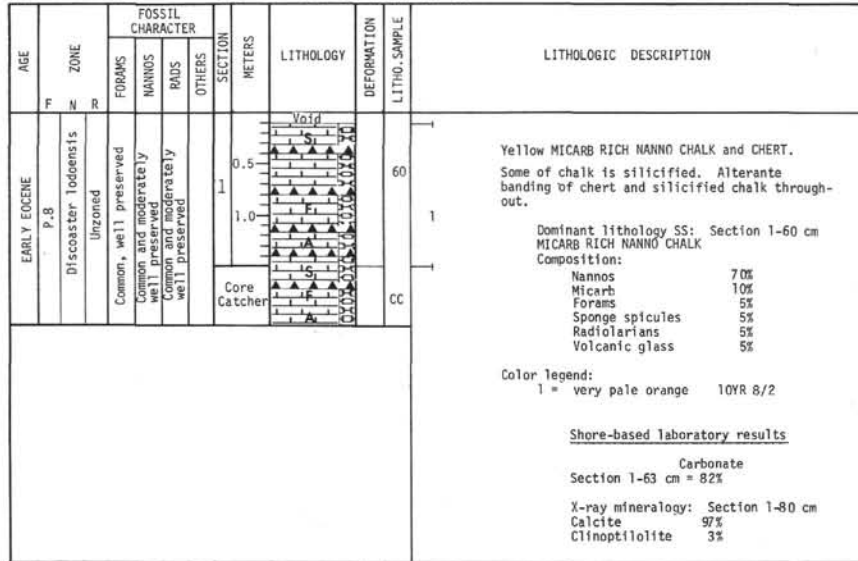


Explanatory notes in chapter 2

Site 220 Hole Core 16 Cored Interval: 288-297

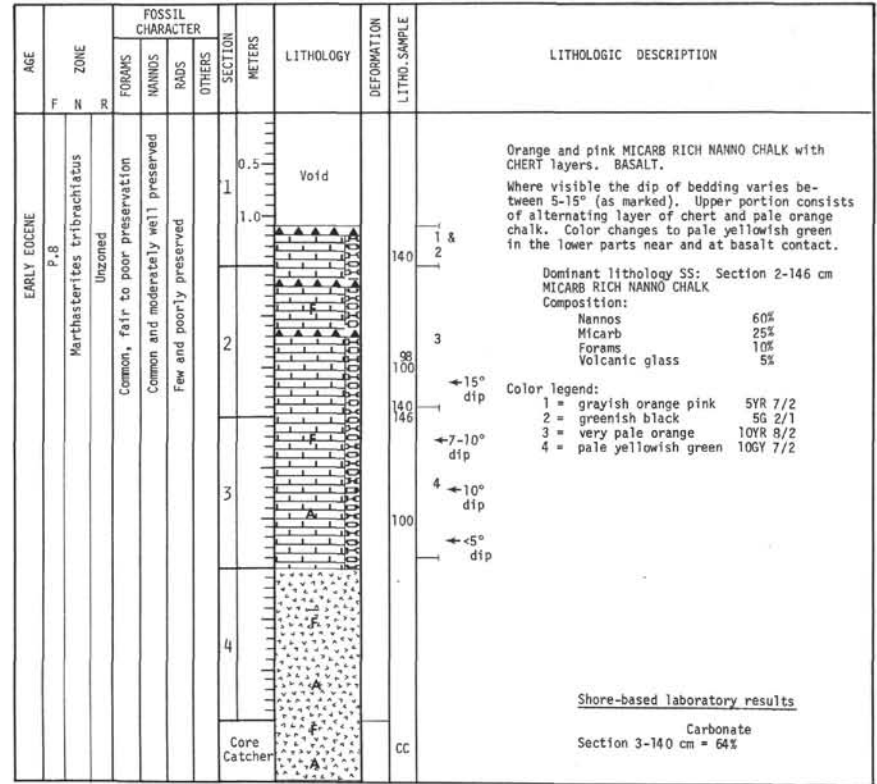


Site 220 Hole Core 17 Cored Interval: 297-306



Explanatory notes in chapter 2

Site 220 Hole Core 18 Cored Interval: 326-330



Explanatory notes in chapter 2

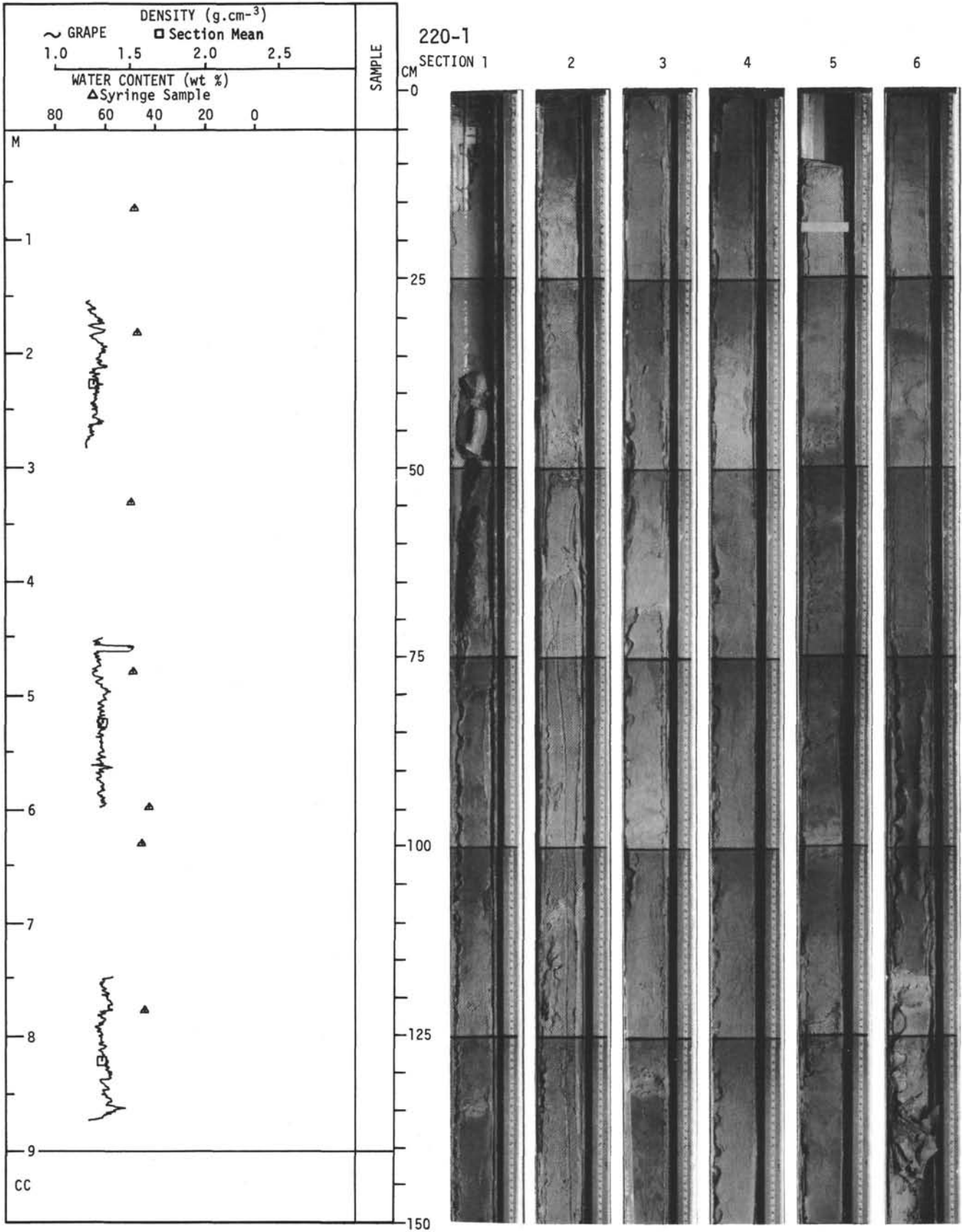
AGE		ZONE			FOSSIL CHARACTER			SECTION METERS	LITHOLOGY	DEFORMATION LITHO. SAMPLE	LITHOLOGIC DESCRIPTION
F	N	R	FORAMS	NANNOS	RADS	OTHERS					
								Void			
							0.5			BASALT with 4 centimeter layer of sediments. Reddish brown to grayish green sediments within the basalt are thinly bedded and well-indurated. Sediment lithology SS: Section 1-43 cm NANNO BEARING MICARB CHALK Composition: Micarb 95% Nannos 3% Forams 2% Sediment lithology SS: Section 1-44 cm NANNO BEARING CHLORITE MICARB CHALK Composition: Micarb 60% Chlorite 25% Nannos 10% Forams 5% * chilled margin	
							1.0				
							2		43 44	*	
							Core Catcher				

AGE		ZONE			FOSSIL CHARACTER			SECTION METERS	LITHOLOGY	DEFORMATION LITHO. SAMPLE	LITHOLOGIC DESCRIPTION
F	N	R	FORAMS	NANNOS	RADS	OTHERS					
								Void			
							0.5			Gray BASALT and green CALCAREOUS CHALK Thin (one-half centimeter thick) dark green chalk layer above partially fractured basalt. Sediment lithology SS: Section 1-90 cm CALCAREOUS CHALK Composition: Authigenic carbonate 100% Nannos Trace	
							1.0				
							Core Catcher		90 CC		

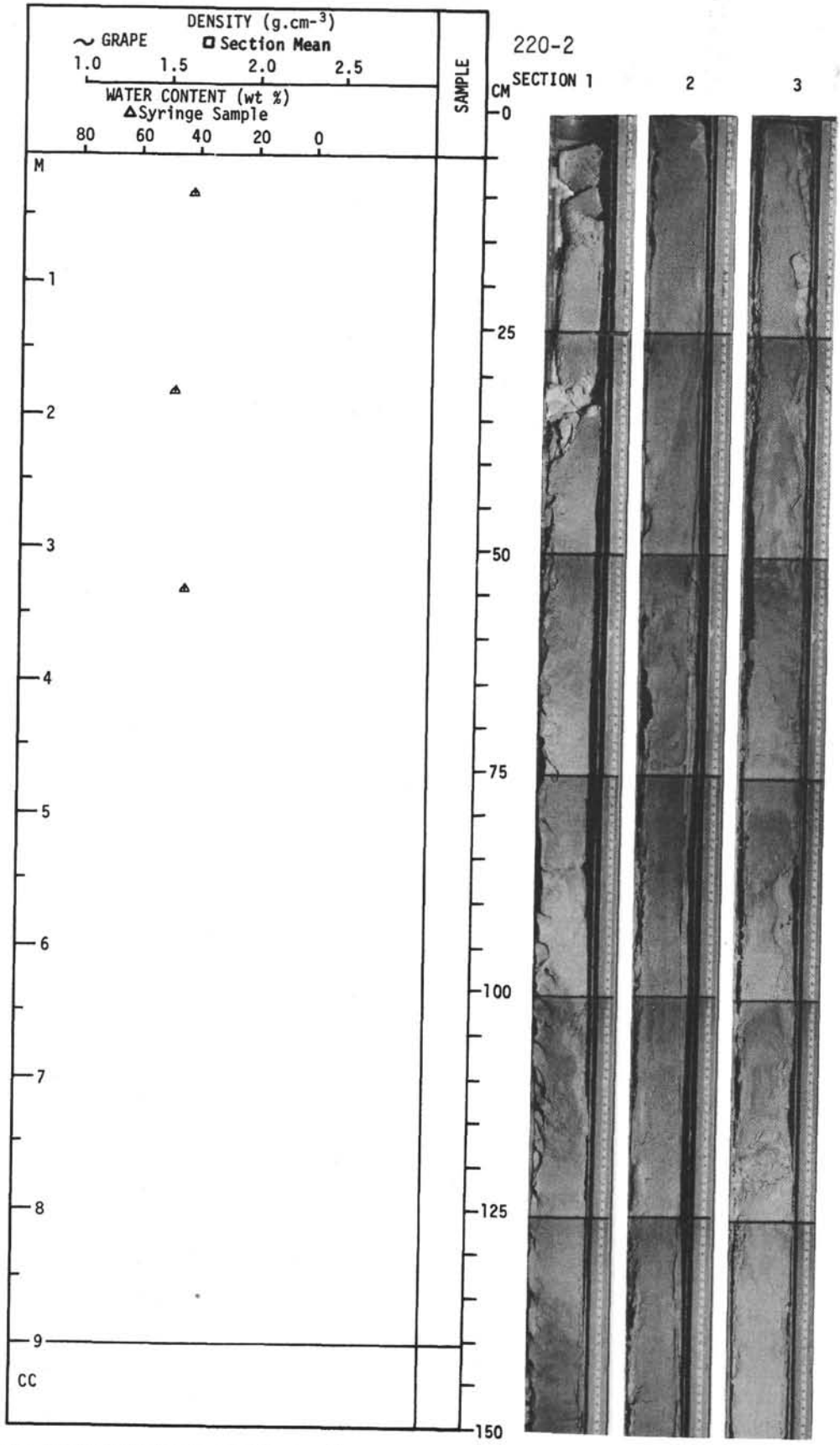
Explanatory notes in chapter 2

AGE		ZONE			FOSSIL CHARACTER			SECTION METERS	LITHOLOGY	DEFORMATION LITHO. SAMPLE	LITHOLOGIC DESCRIPTION
F	N	R	FORAMS	NANNOS	RADS	OTHERS					
								Void			
							0.5			BASALT Basalt is fractured and exhibits chilled margins. A number of different colored veins are present. Some are calcite filled. Remarks: From the drill bit, pieces of basalt and small lumps of brown and green sediments were recovered. Examination reveals that the sediments came from higher in the hole.	
							1.0				
							2			* * * * * *	
							Core Catcher			* chilled margin.	

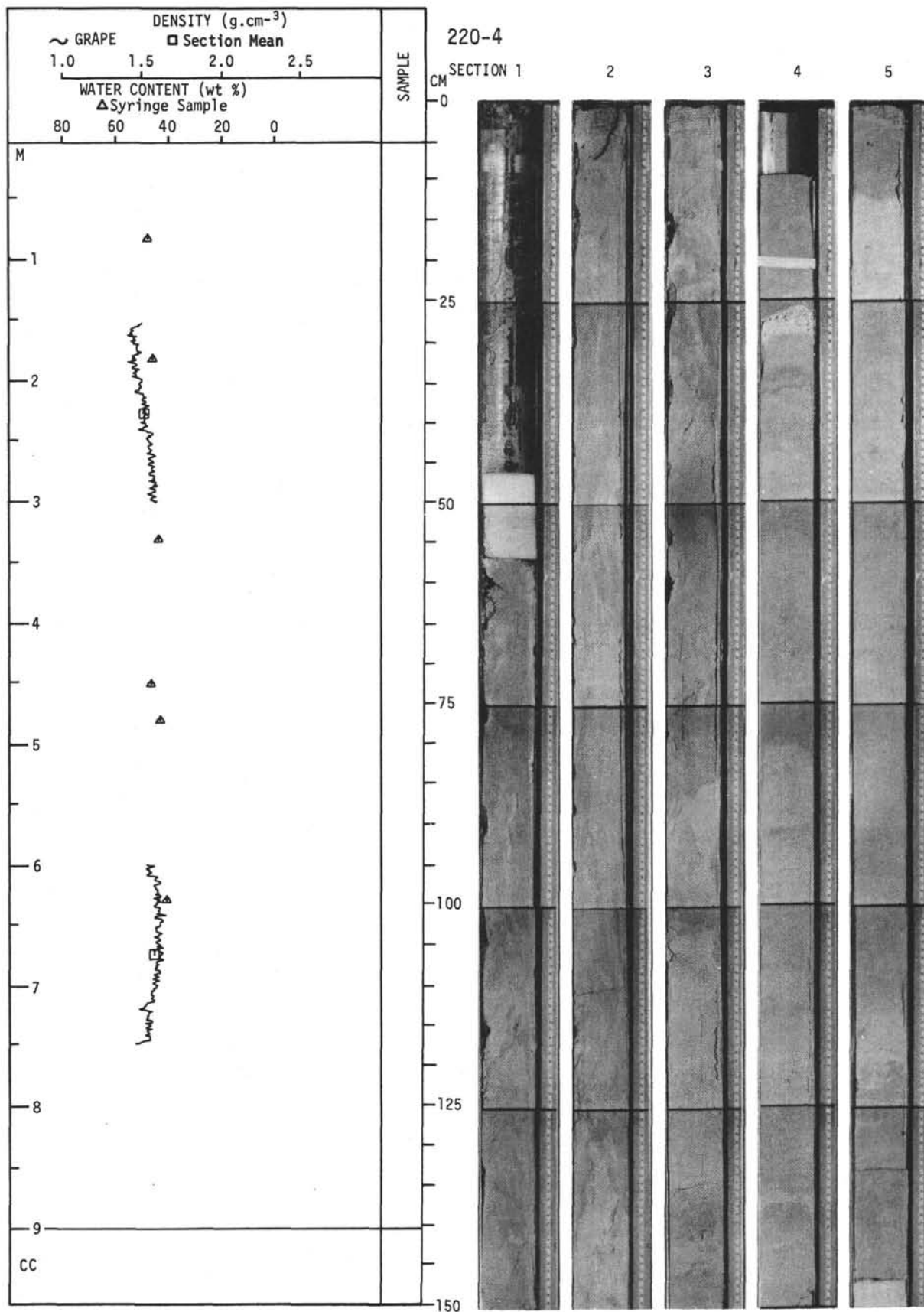
Explanatory notes in chapter 2



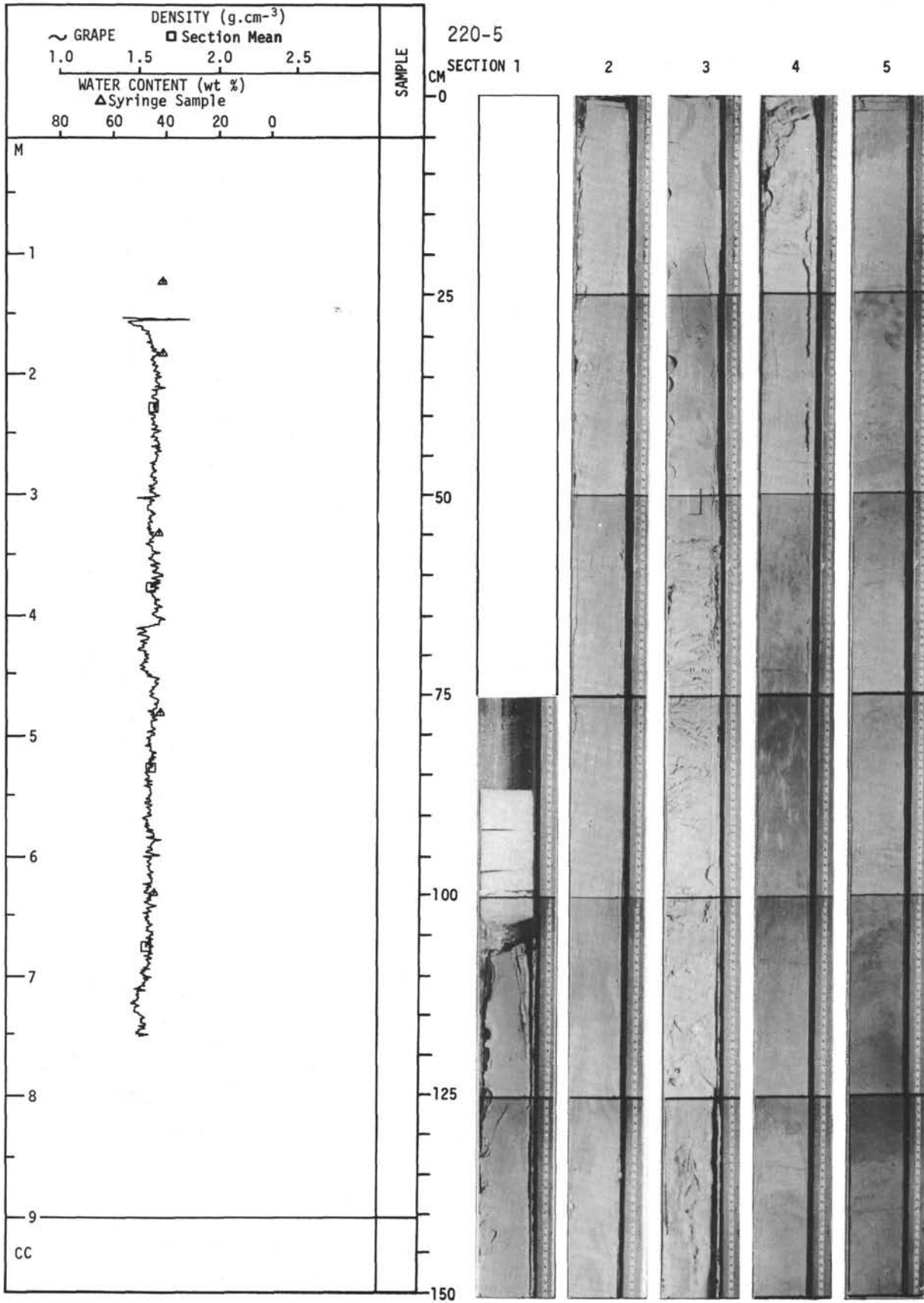
For Explanatory Notes, see Chapter 2



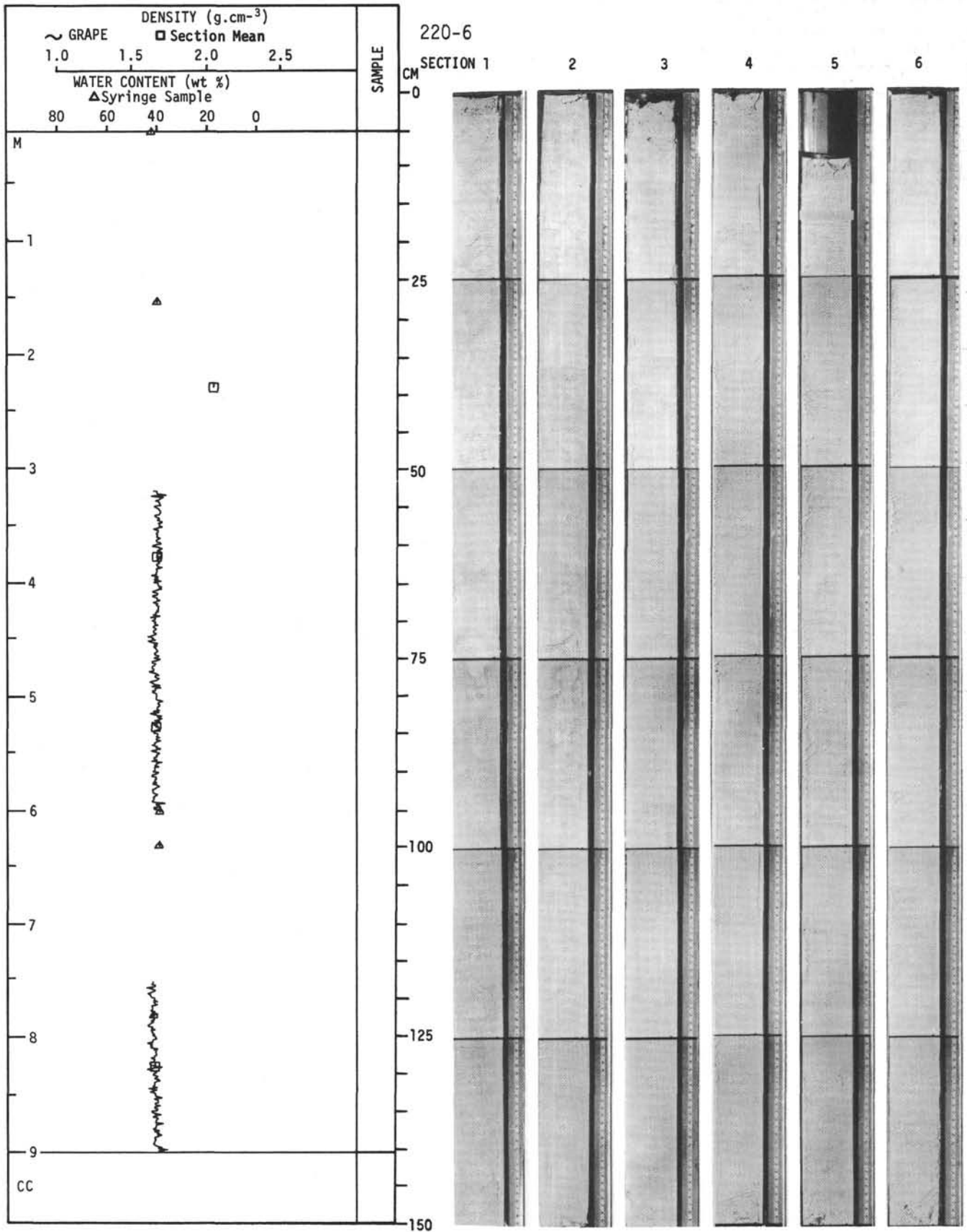
For Explanatory Notes, see Chapter 2



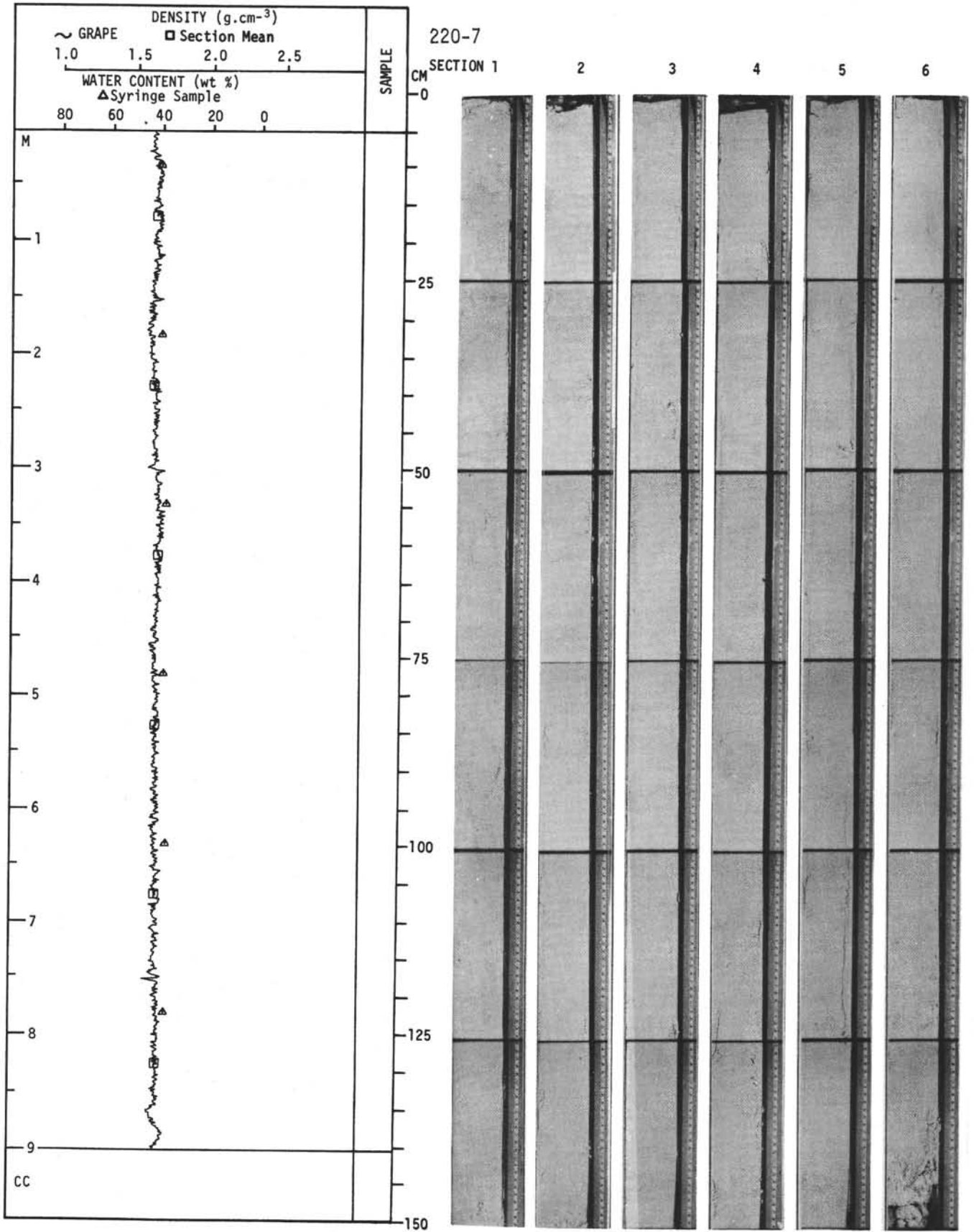
For Explanatory Notes, see Chapter 2



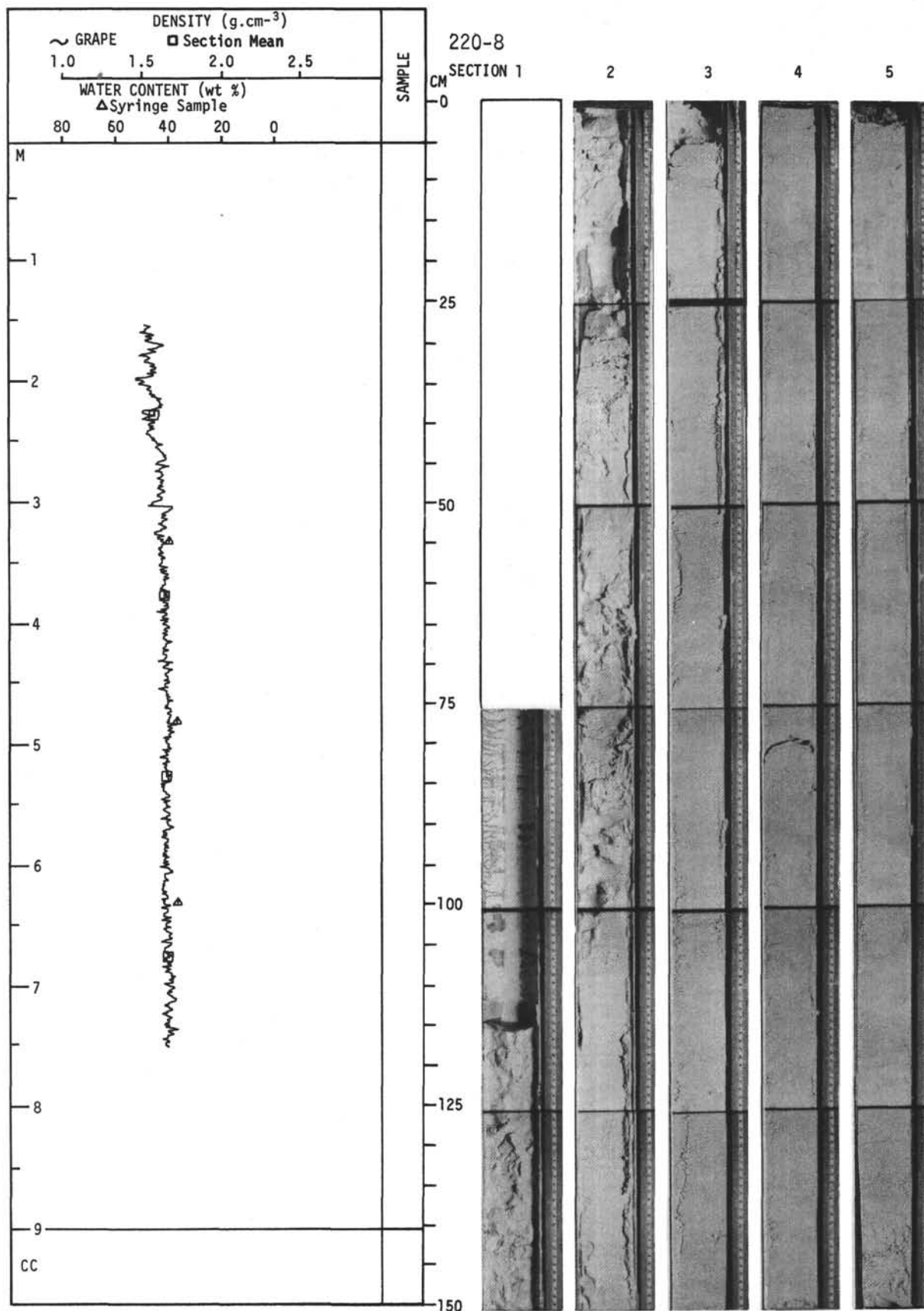
For Explanatory Notes, see Chapter 2



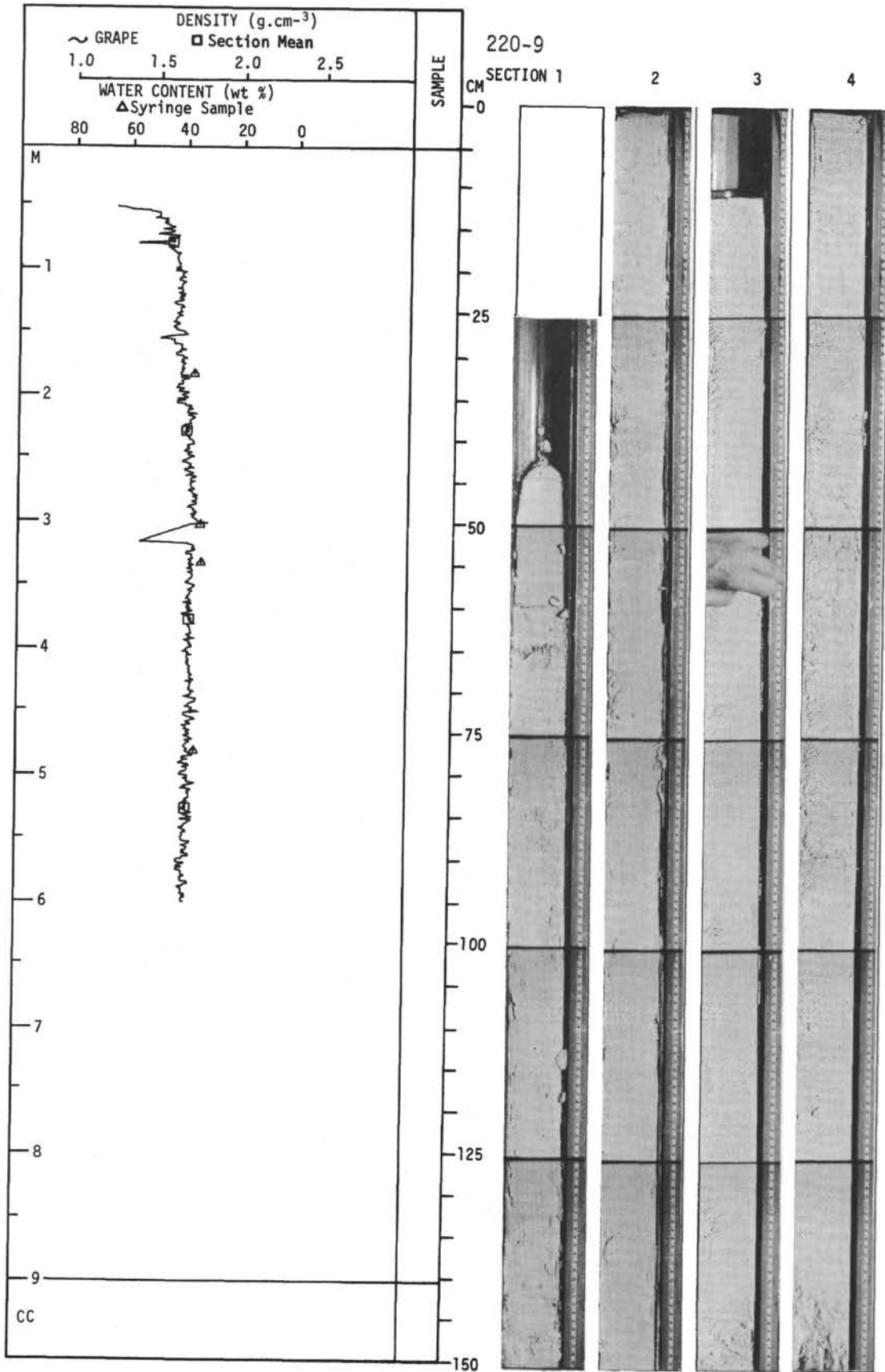
For Explanatory Notes, see Chapter 2



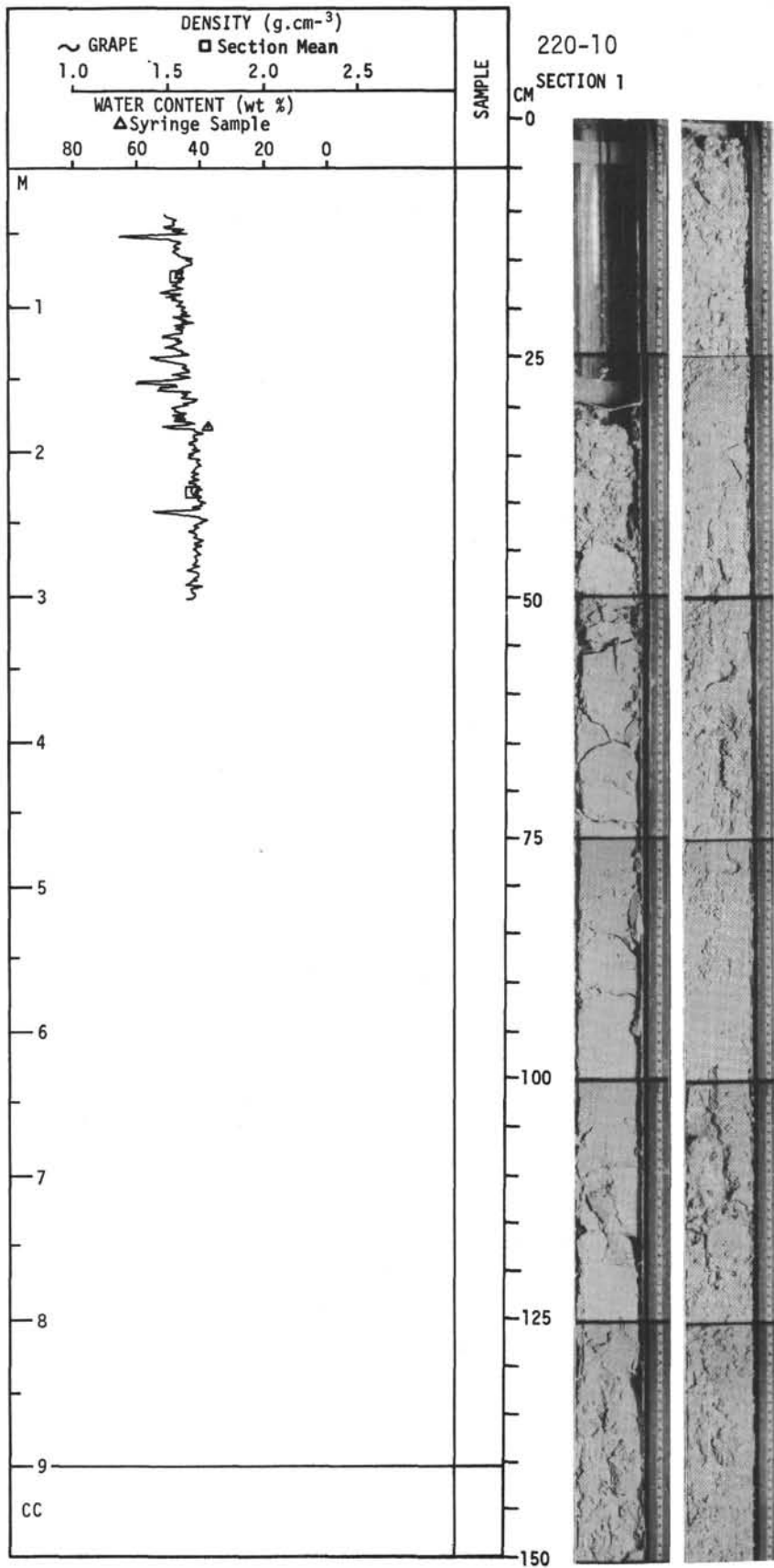
For Explanatory Notes, see Chapter 2



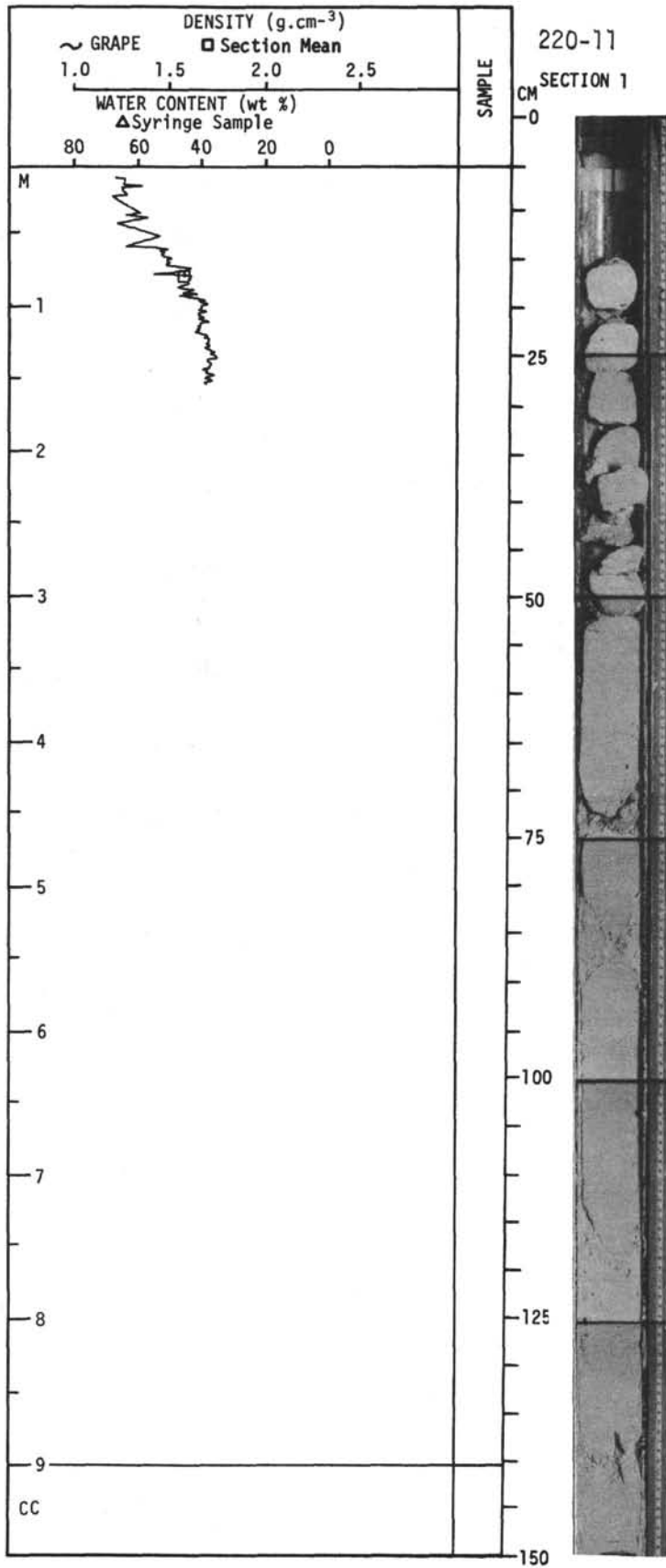
For Explanatory Notes, see Chapter 2



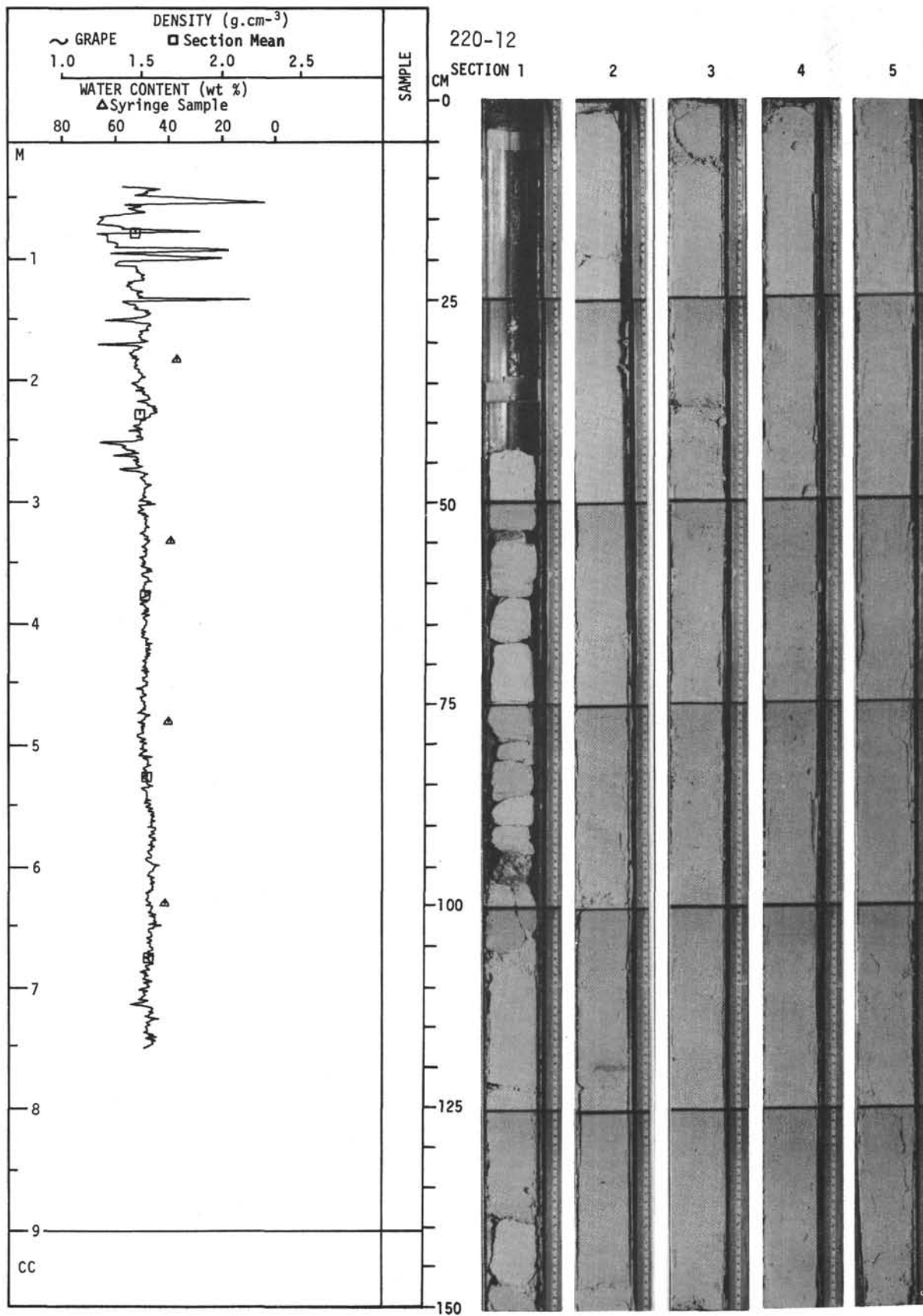
For Explanatory Notes, see Chapter 2



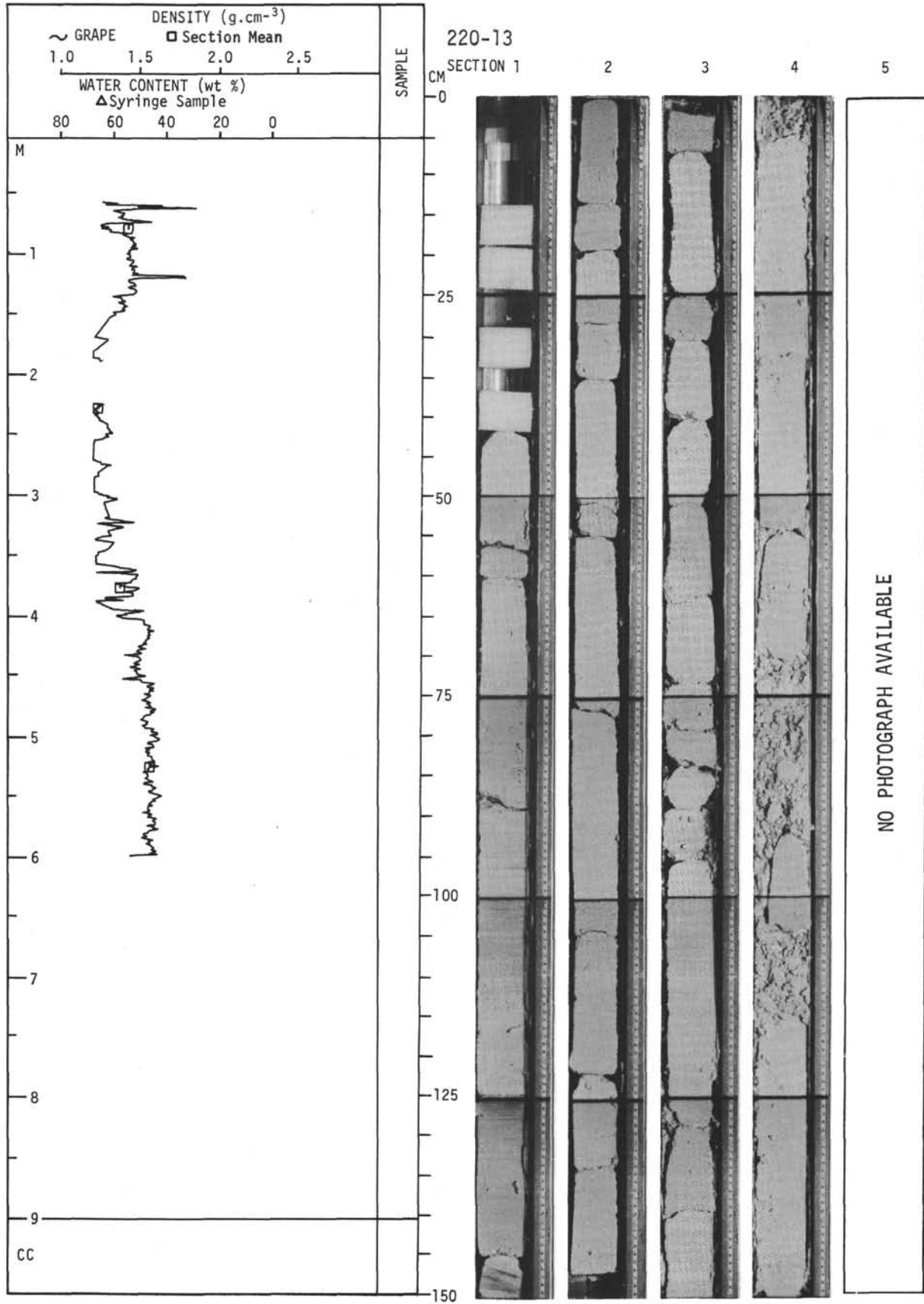
For Explanatory Notes, see Chapter 2



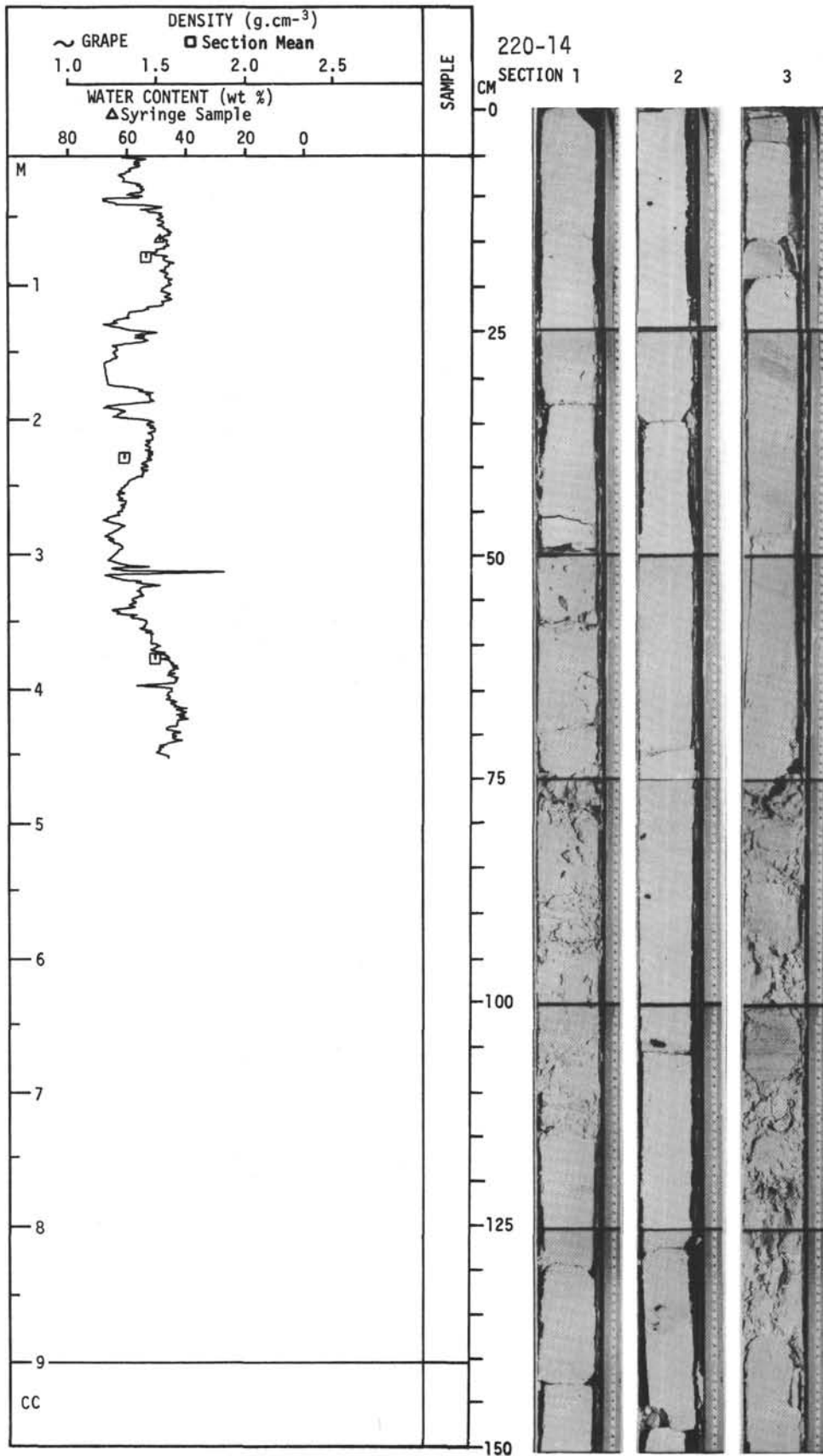
For Explanatory Notes, see Chapter 2



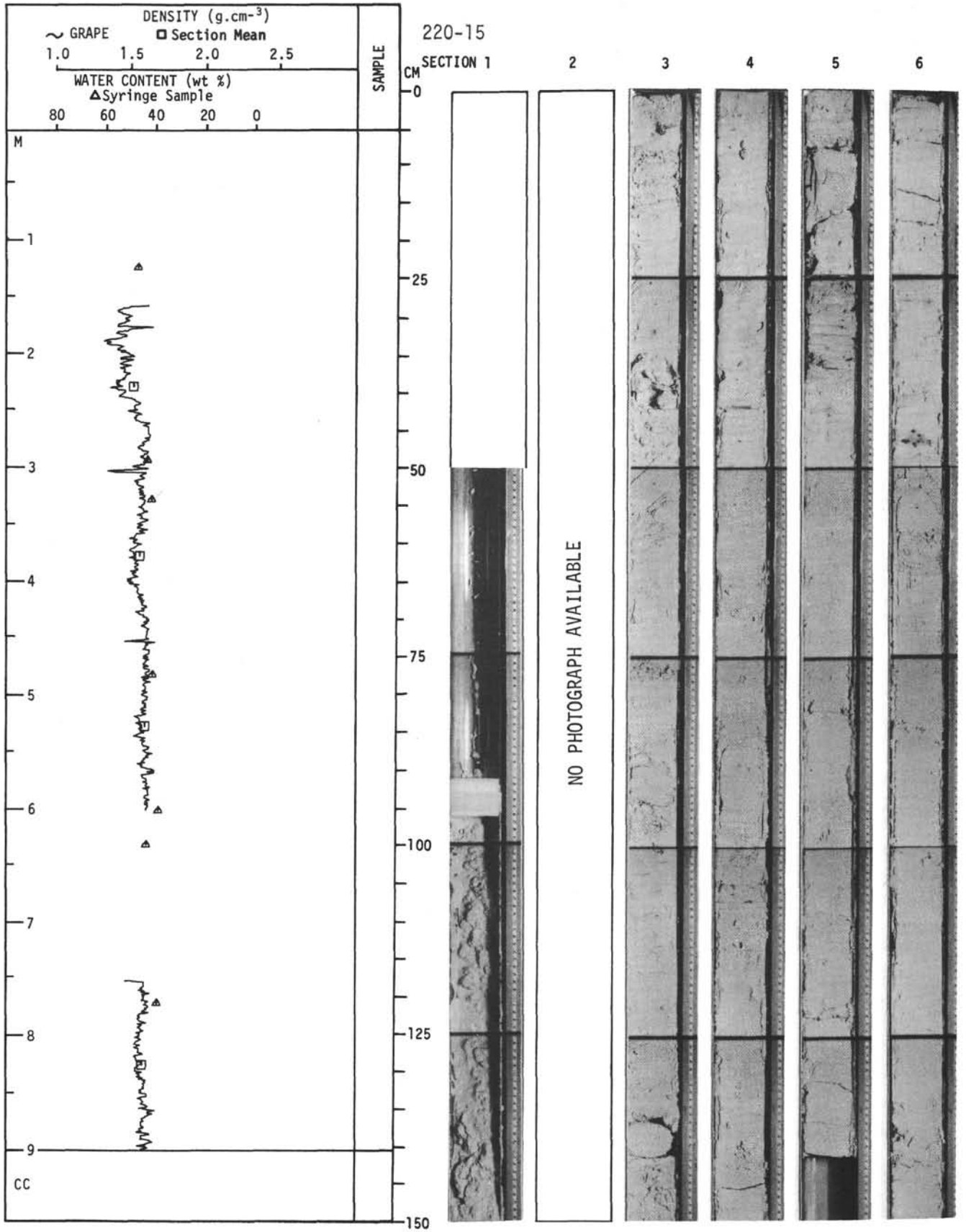
For Explanatory Notes, see Chapter 2



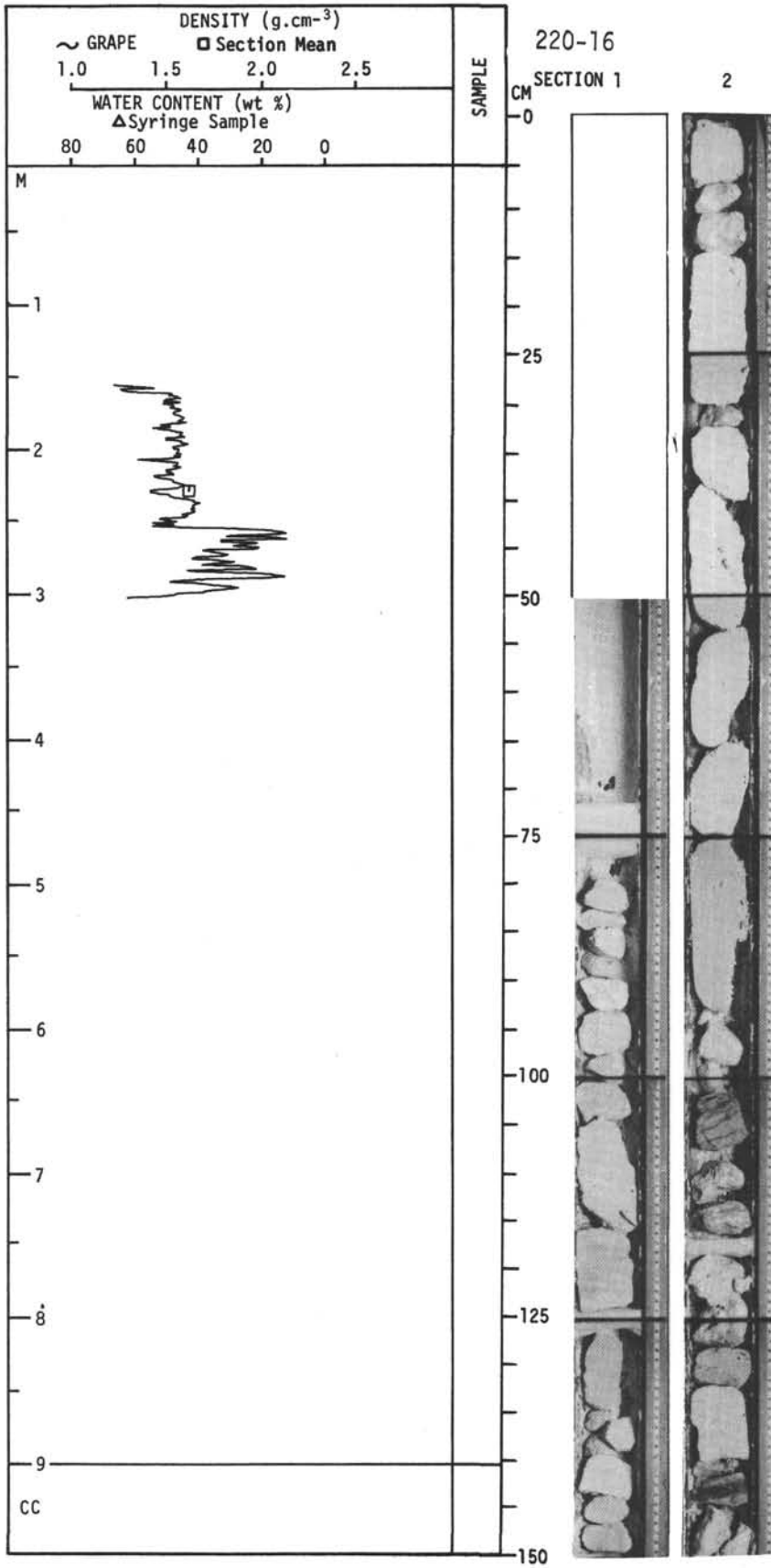
For Explanatory Notes, see Chapter 2



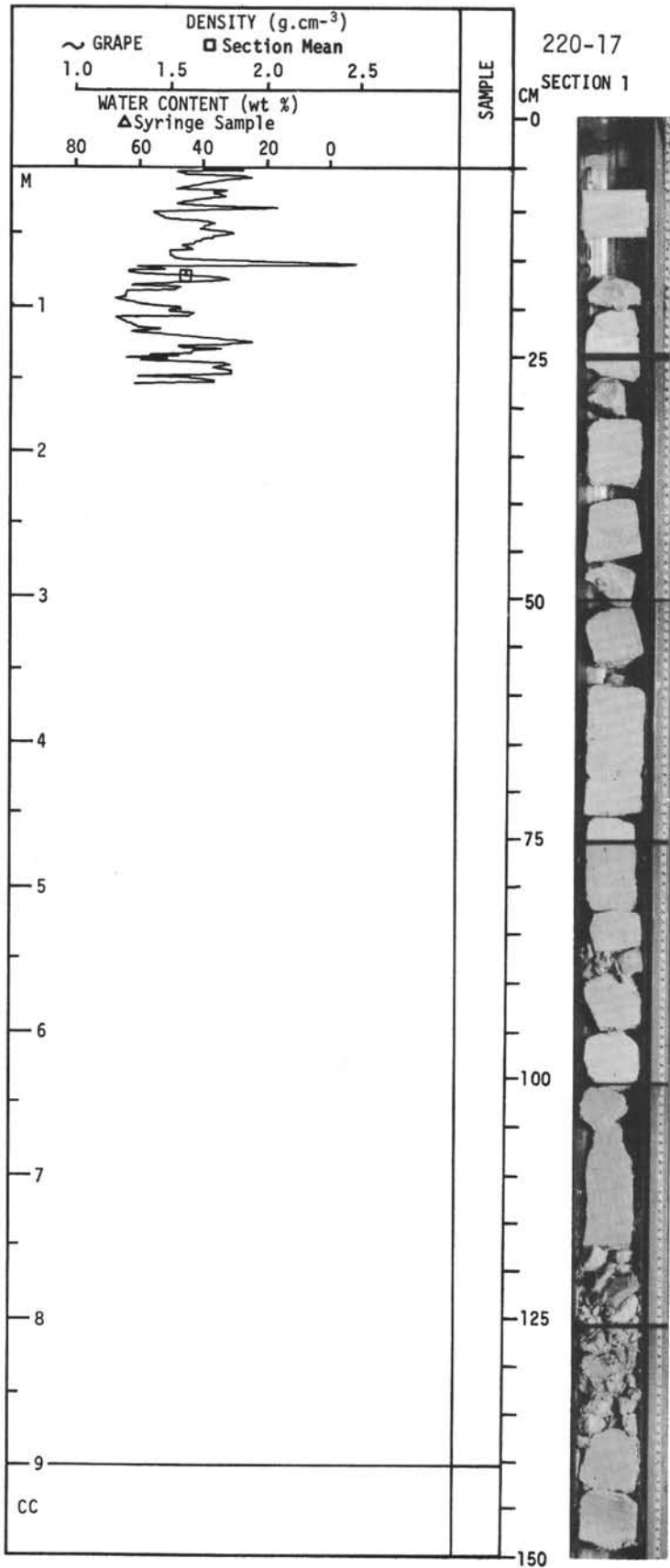
For Explanatory Notes, see Chapter 2



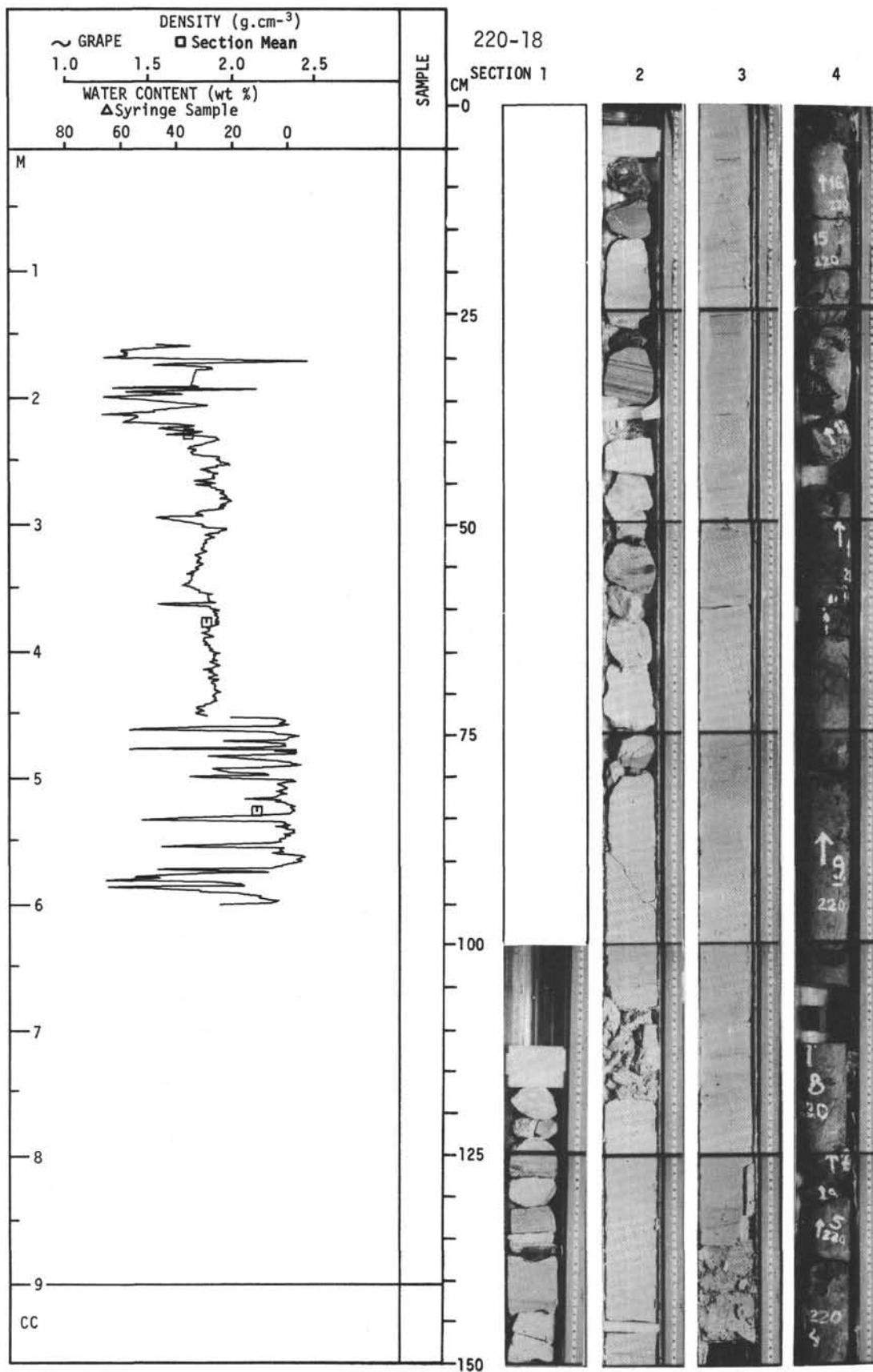
For Explanatory Notes, see Chapter 2



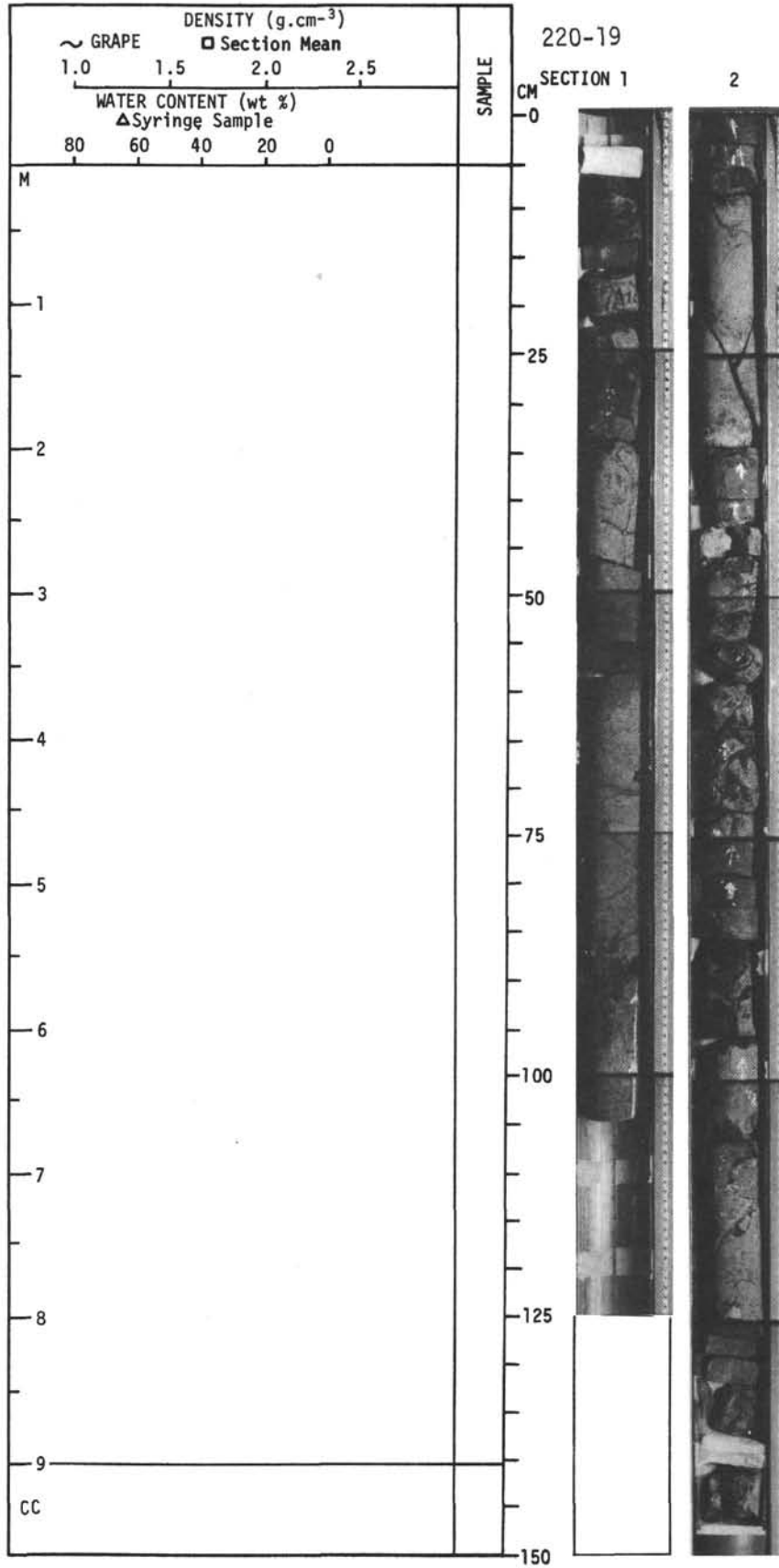
For Explanatory Notes, see Chapter 2



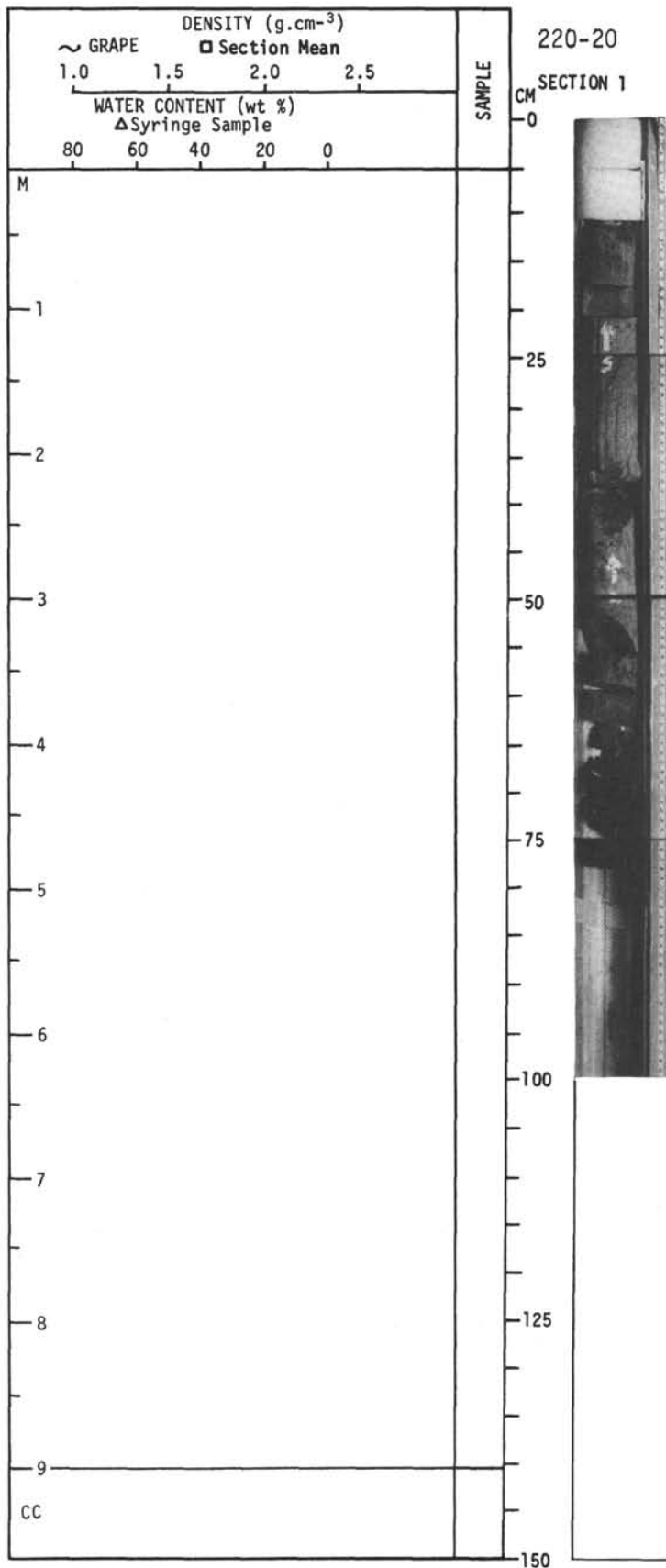
For Explanatory Notes, see Chapter 2



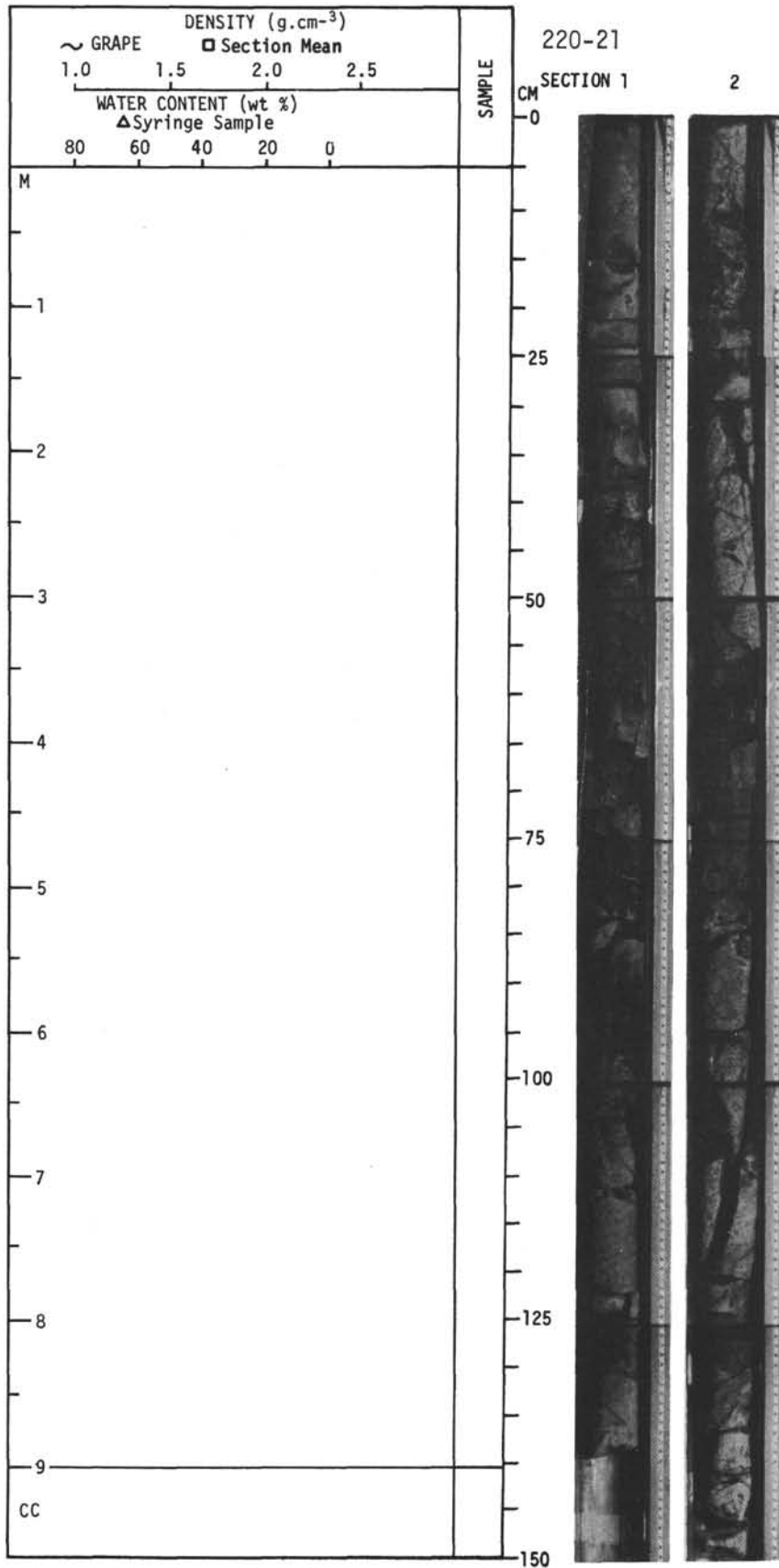
For Explanatory Notes, see Chapter 2



For Explanatory Notes, see Chapter 2



For Explanatory Notes, see Chapter 2



For Explanatory Notes, see Chapter 2